JASN

J Am Soc Nephrol. 2015 Aug; 26(8): 1855–1876.
Published online 2014 Dec 5.
doi: 10.1681/ASN.2014010065: 10.1681/ASN.2014010065

PMCID: PMC4520158
PMID: 25479966

Evidence of a Role for Fibroblast Transient Receptor Potential Canonical 3 Ca^{2+} Channel in Renal Fibrosis

Youakim Saliba,[*] Ralph Karam,[*] Viviane Smayra,[†] Georges Aftimos,[‡] Joel Abramowitz,[§] Lutz Birnbaumer,[§] and Nassim Farès[✉*]

[*]Physiology and Pathophysiology Research Laboratory, Pole of Technology and Health, Faculty of Medicine and
[†]Faculty of Medicine, Saint Joseph University, Beirut, Lebanon;
[‡]Department of Anatomopathology, National Institute of Pathology, Baabda, Lebanon; and
[§]Laboratory of Neurobiology, National Institute of Environmental Health Sciences, Research Triangle Park, North Carolina
[✉]Corresponding author.
V.S. and G.A. contributed equally to this work.
Correspondence: Prof. Nassim Farès, Laboratory of Physiology and Pathophysiology Research Laboratory, Faculty of Medicine, Saint Joseph University, Beirut, Lebanon. Email: nassim.fares@usj.edu.lb

Received 2014 Jan 15; Accepted 2014 Sep 23.

Abstract

Transient receptor potential canonical (TRPC) Ca^{2+}-permeant channels, especially TRPC3, are increasingly implicated in cardiorenal diseases. We studied the possible role of fibroblast TRPC3 in the development of renal fibrosis. *In vitro*, a macromolecular complex formed by TRPC1/TRPC3/TRPC6 existed in isolated cultured rat renal fibroblasts. However, specific blockade of TRPC3 with the pharmacologic inhibitor pyr3 was sufficient to inhibit both angiotensin II- and 1-oleoyl-2-acetyl-*sn*-glycerol–induced Ca^{2+} entry in these cells, which was detected by fura-2 Ca^{2+} imaging. TRPC3 blockade or Ca^{2+} removal inhibited fibroblast proliferation and myofibroblast differentiation by suppressing the phosphorylation of extracellular signal-regulated kinase (ERK1/2). In addition, pyr3 inhibited fibrosis and inflammation-associated markers in a noncytotoxic manner. Furthermore, TRPC3 knockdown by siRNA confirmed these pharmacologic findings. In adult male Wistar rats or wild-type mice subjected to unilateral ureteral obstruction, TRPC3 expression increased in the fibroblasts of obstructed kidneys and was associated with increased Ca^{2+} entry, ERK1/2 phosphorylation, and fibroblast proliferation. Both TRPC3 blockade in rats and TRPC3 knockout in mice inhibited ERK1/2 phosphorylation and fibroblast activation as well as myofibroblast differentiation and extracellular matrix remodeling in obstructed kidneys, thus ameliorating tubulointerstitial damage and renal fibrosis. In conclusion, TRPC3 channels are present in renal fibroblasts and control fibroblast proliferation, differentiation, and activation through Ca^{2+}-mediated ERK signaling. TRPC3 channels might constitute important therapeutic targets for improving renal remodeling in kidney disease.

Keywords: fibroblast, renal fibrosis, ion channel, calcium, kidney disease, cell, signaling

It is estimated that >14% of the adult population has some degree of CKD, and the prevalence of patients with ESRD is increasing worldwide.[1,2] Most progressive renal dysfunctions eventually lead to renal fibrosis, regardless of the underlying disease.[3–7] Therefore, a better understanding of the pathologic mechanisms and signaling pathways contributing to renal fibrosis is essential for developing new treatment strategies.[8]

Renal fibrosis (more specifically, interstitial fibrosis) is characterized by aberrant growth and proliferation of renal fibroblasts. The activated fibroblast undergoes a phenotypic change to a myofibroblast, which is characterized by α-smooth muscle actin (α-SMA) expression, as well as increased production of cytokines and extracellular matrix (ECM) components, such as collagen and fibronectin (Fn).[9–11] The myofibroblast is the key cellular mediator of fibrosis, and its presence correlates with the extent of tubulointerstitial damage. Other cellular events occur in renal fibrosis, such as tubular epithelial-to-mesenchymal transition (EMT), cell apoptosis, and monocyte/macrophage and T-cell infiltration[6,12]; it is noteworthy that EMT is still a debatable phenomenon.[13–20]

Calcium (Ca^{2+}) is an important signaling molecule implicated in diverse cellular functions, such as differentiation, gene expression, cell proliferation, growth, and death,[21,22] and it plays a significant role in regulating fibroblast functions.[23] Transient receptor potential canonical (TRPC) channels are voltage-independent, nonselective Ca^{2+} channels.[24] Among this channel family, TRPC3 has been increasingly implicated in many forms of disease. TRPC3 is a receptor-operated cation channel that can be activated by angiotensin II (Ang II) or endothelin I through stimulation of their corresponding receptors and secondary generation of diacylglycerol (DAG).[25,26] TRPC3 is upregulated in kidney and monocytes from patients with hypertension and correlates with proinflammatory cytokines.[27–31] Increased TRPC3 channel protein expression is found in human monocytes from patients with CKD,[32] and association of TRPC3 with hypertension is increasingly being reported.[33–35] TRPC3 also promotes cardiac hypertrophy through calcineurin and NF of activated T cells[36–39] and mediates a proarrhythmic Ca^{2+} entry in cardiac myocytes.[40,41] The TRPC3-selective inhibitor, ethyl-1-(4-(2,3,3-trichloroacrylamide)phenyl)-5-(trifluoromethyl)-^{1}H-pyrazole-4-carboxylate (pyr3), is reported to block cardiac hypertrophy in mice subjected to pressure overload, with a marked selectivity for TRPC3 over other TRPs from the same family,[42] and prevent stent-induced arterial remodeling.[43] More recently, TRPC3 has been found in human cardiac fibroblasts and regulated cell proliferation and differentiation in atrial fibrillation.[44,45] Few other studies reported the presence of TRPC channels in normal rat kidney cell lines[46,47] and identified their localization in the adult rat and human kidney.[48–51] TRPC3 is also responsible for transepithelial Ca^{2+} flux in principal cells of the renal collecting duct[52–54]; however, a clear functional *in vivo* role of such channels remains totally unclear, especially in the diseased kidney. Therefore, it is important to study the role of TRPC3 in renal fibroblasts and its role in the pathogenesis of renal fibrosis associated with kidney disease.

The model of unilateral ureteral obstruction (UUO) that is used in our study generates progressive renal fibrosis that is independent of hypertension or systemic immune disease.[55] The UUO maneuver mimics, in an accelerated manner, the different stages of obstructive nephropathy leading to tubulointerstitial fibrosis: cellular infiltration, tubular proliferation and apoptosis, EMT, myofibroblast accumulation, increased ECM deposition, and tubular atrophy.[55–58] In this study, we examined the role of TRPC3 in renal fibroblasts and evaluated the therapeutic efficiency of TRPC3 inhibition in obstructive nephropathy in rat and TRPC3 knockout ($TRPC3^{-/-}$) mouse UUO models.

Results

Functional TRPC3 in Renal Fibroblasts

Rat renal fibroblasts expressed high levels of TRPC3 channels; the protein band disappeared in the protein lysate of TRPC3$^{-/-}$ mice kidneys, confirming the specificity of the detected channel protein band (Figure 1A). These channels were then tested for whether they contribute to Ca^{2+} entry in these cells. Because TRPC3 is physiologically activated by DAG,[59,60] the DAG analog 1-oleoyl-2-acetyl-*sn*-glycerol (OAG) and the DAG generating Ang II were used to stimulate TRPC3 Ca^{2+} entry directly and indirectly, respectively. Because previous reports showed a dose-dependent effect of pyr3 on cellular Ca^{2+} entries,[42,43] different concentrations of this TRPC3 inhibitor were first tested on OAG-induced Ca^{2+} entry (Figure 1B). Minor inhibitory effects appeared with 0.1 and 1 μM pyr3, whereas the largest inhibition was observed with 10 μM (Figure 1B). Higher concentrations were not tested, because this latter one has been consistently shown to exhibit maximal inhibitory effects on TRPC3 channel activity without affecting other TRPC protein isoforms.[42]

Large Ca^{2+} entries were observed after extracellular Ca^{2+} addition in control cells, and DMSO did not have any effect. OAG-induced Ca^{2+} entry significantly diminished in rate and amplitude when preincubating cells with pyr3, and more pronounced inhibition was noted with the nonselective blockers SKF96365, the lanthanide Gd^{3+}, and 2-aminoethoxydiphenyl borate (2-APB) (Figure 1, C–E). When pyr3 was acutely administered to fibroblasts after OAG stimulation, Ca^{2+} entry amplitude began to fall and reached a significantly lower plateau. Acute addition of SKF96365, Gd^{3+}, or 2-APB led to a further drop in Ca^{2+} entries with faster rates of inhibition (Figure 1, F–H).

TRPC3 channels were then indirectly activated through application of inositol trisphosphate-generating Ang II; an initial small peak in fura-2 signal indicated intracellular Ca^{2+} mobilization by Ang II, which was followed by an important Ca^{2+} entry after readdition of extracellular Ca^{2+} (Figure 2A). TRPC3 inhibitor abolished the increase in Ca^{2+} entry without affecting initial Ca^{2+} mobilization (Figure 2, A and B), and DMSO did not produce any noticeable effect (Figure 2, A and B). TRPC channel blockers, such as SKF96365, Gd^{3+}, and 2-APB, led to further Ca^{2+} entries inhibition (Figure 2, B and C), with 2-APB also inhibiting initial Ca^{2+} mobilization by Ang II (data not shown). Acute addition of pyr3 resulted in similar Ca^{2+} entry abrogation with significantly lower amplitude, whereas SKF96365, Gd^{3+}, and 2-APB produced even more inhibition (Figure 2, D–F).

Because manganese (Mn^{2+}) ions are used as Ca^{2+} surrogates and seem to traverse most Ca^{2+}-permeable channels,[25,61,62] basal cation entry was further recorded using the quenching of fura-2 fluorescence by Mn^{2+} technique. Cultured renal fibroblasts were first perfused by Mn^{2+} followed by either OAG or Ang II, which resulted in large increases in fura-2 fluorescence quenching (Supplemental Figure 1). Chronic or acute addition of pyr3 to the cells resulted in significant decreases in Mn^{2+} quench rates, whereas the ionophore ionomycin resulted in complete fura-2 fluorescence quenching (Supplemental Figure 1).

A series of fibroblasts was subjected to on and off extracellular Ca^{2+} switches to identify the existence of a possible basal Ca^{2+} entry. However, Ca^{2+} readdition after EGTA did not result in a significant increase in intracellular Ca^{2+}, and pyr3 did not have any noticeable effect (Supplemental Figure 2, A and B). Maximum and minimum fluorescence values that could be obtained in our experimental conditions were also checked by consecutive ionomycin and EGTA addition (Supplemental Figure 2, C and D).

Finally, fura-2 fluorescence was monitored over time without any significant decrease in values, indicating the absence of dye leak from the cells (Supplemental Figure 3).

TRPC3 Inhibition Blocked Renal Fibroblasts Proliferation

Immunocytochemistry revealed (at day 0 of renal fibroblasts culture) a strong expression of mesenchymal cell marker vimentin, with no presence of epithelial marker cytokeratin (Supplemental Figure 4, A, B, and E). At day 5 of culture, vimentin staining strongly reacted with the abundant intermediate filaments of the

cultured cells with still no expression of cytokeratin (Supplemental Figure 4, C–E), indicating consistently pure renal fibroblastic cell preparations without contamination with tubular epithelial cells. As expected, fibroblasts presented more cell spreading at day 5 of culture. Furthermore, specific markers for each possible contaminating cell type were chosen as previously and widely described.[63–69] Indeed, expressions of clusters of differentiation of CD31, CD68, and CD11c as well as kidney-specific cadherin 16, EpCAM, and E-cadherin were hardly detected in the cultured cells at days 0 and 5 compared with total kidney, indicating the absence of contaminating endothelial cells, monocytes/macrophages, dendritic cells, and tubular epithelial cells (Supplemental Figure 4F); this confirms the immunocytochemistry results as to the purity of the culture preparations.

MTT cell proliferation assay showed a pyr3 dose-dependent inhibition of renal fibroblasts proliferation with a most prominent effect of the 10 μM concentration (Figure 3A). Cell counting further confirmed these results with marked decreases in cell numbers with TRPC3 blockade compared with DMSO-treated or control nontreated cells (Figure 3B). Cell cycle-negative regulators p53 and p21 were upregulated with TRPC3 inhibition, whereas positive regulators that are normally expressed in proliferating cells (Ki67 and proliferating cell nuclear antigen [PCNA]) presented diminished expression under TRPC3 blockade (Figure 3, C and D).

Fibroblast Activation through TRPC3-Mediated Ca^{2+} Entry and Extracellular Signal-Regulated Kinase 1/2

TRPC3-mediated activation of renal fibroblasts was then analyzed to check if TRPC3 Ca^{2+} signaling was important and essential in triggering the mitogen-activated protein kinase–extracellular signal-regulated kinase (ERK) pathway. TRPC3 blockade by pyr3 inhibited ERK1/2 phosphorylation compared with nontreated control and DMSO-treated cells (Figure 4, A and B). Low extracellular Ca^{2+} (0.2 mM) also inhibited ERK1/2 phosphorylation compared with control conditions (2 mM Ca^{2+}) (Figure 4, A and B). Total ERK was not affected by either treatment (Figure 4, A and B). The importance of the ERK pathway in fibroblast activation and proliferation was further substantiated by the selective ERK pathway inhibitors PD98059 and U0126 that diminished ERK phosphorylation and fibroblasts proliferation (Figure 4, C–E). Finally, lowering extracellular Ca^{2+} suppressed cell proliferation, showing the importance of Ca^{2+} influx in this cellular process (Figure 4E).

TRPC3 Inhibition Suppressed Myofibroblast Differentiation, Fibrosis, and Inflammation-Associated Phenotype through ERK1/2

Ca^{2+} influx and ERK phosphorylation abrogation effect on the phenotype and secretory profile of renal fibroblasts with TRPC3 blockade was studied. Cells treated with pyr3 showed significantly less differentiation into myofibroblasts, which was shown by the net decrease of α-SMA that characterizes this type of cells (Figure 5A). ECM components, such as collagens 1, 3, and 4 and Fn1 expression, as well as regulators, like matrix metalloproteinase 2 (MMP2), MMP9, and tissue inhibitor of metalloproteinase 1 (TIMP1), diminished with TRPC3 blockade along with the fibrogenic activator connective tissue growth factor (Figure 5B); pyr3-treated fibroblasts showed decreased expressions of the monocyte recruiting chemokine MCP1 with suppression of the prostanoid and leukotriene pathways shown by diminished cyclooxygenase 2 and arachidonate 5-lipoxygenase expressions (Figure 5C). Secretions of inflammatory and fibrotic cytokines, such as IL-1, IL-6, and TGF-β1, as well as collagen synthesis were significantly reduced with TRPC3 blockade (Figure 5, D and E). To further confirm ERK1/2 necessity for α-SMA, collagen, and cytokines production, treatment of renal fibroblasts cultures with PD98059 resulted in significant inhibition of α-SMA, collagens 1, 3, and 4, and Fn1 expressions as well as IL-1 and IL-6 secretions (Figure 5, F and G).

Noncytotoxic Effects of TRPC3 Blockade on Renal Fibroblasts

To exclude the possibility that the antiproliferative, antifibrotic effects of TRPC3 blockade were mediated by cellular toxicity with a general killing phenomenon, the Trypan blue exclusion test was carried out to examine the viability of the renal fibroblasts after pyr3 treatment. The results indicated that TRPC3 blockade with different pyr3 concentrations did not have any significant cytotoxicity (Figure 6, A–E). Additional confirmation was done by studying the expression of relatively stable genes that should not be affected with pyr3 treatment; stable expression of endogenous markers, such as β-actin, tata box protein, and ribosomal protein L32, was noted, validating the absence of cell killing with global genes downregulations (Figure 6, F–H). As a positive control, H_2O_2 treatment resulted in high cytotoxicity, which was shown by the Trypan blue total cellular intake (Figure 6, A and E).

TRPC3 Knockdown Suppresses Fibroblast Activation, Proliferation, and Differentiation

TRPC3 was knocked down by specific siRNA in the cultured rat renal fibroblasts, and the relative protein expression significantly decreased after 48 hours of transfection compared with the nonspecific scrambled siRNA and control nontransfected cells (Figure 7A). Renal fibroblasts transfected with cy3-TRPC3 were selected under specific fluorescence filters, and Ca^{2+} influx was recorded after stimulation with either OAG or Ang II. TRPC3 downregulation abrogated Ca^{2+} influx in both stimulations (Figure 7B). This Ca^{2+} influx inhibition was accompanied by attenuated cell proliferation, which was shown by less reactivity to MTT assay and smaller cell numbers (Figure 7, C and D). TRPC3 downregulation suppressed α-SMA expression and hence, myofibroblast differentiation and ERK1/2 phosphorylation with no effect on total ERK expression levels (Figure 7E). The activated fibrotic and inflammatory profiles of renal fibroblasts were suppressed by TRPC3 knockdown, which was shown by reductions of collagen synthesis (Figure 7F) as well as TGF-β1, IL-1, and IL-6 secretions (Figure 7G).

Characterization of the Expression, Subunit Composition, and Function of TRPC Channel Isoforms in Rat Renal Fibroblasts

The possible contribution of other TRPC isoforms to the above-described Ca^{2+} entries and cellular effects was evaluated. Other than TRPC3, freshly isolated renal fibroblasts expressed TRPC1 and -6 on both mRNA and protein levels; however, their relative expressions were less than TRPC3 (Figure 8, A and B). TRPC4 mRNA was barely detected, whereas TRPC2, -5, and -7 were not (Figure 8A). TRPC1, -3, and -6 were present in the same macromolecular complex as revealed by coimmunoprecipitation (Figure 8C). Next, specific TRPC isoform knockdowns were performed to study the functional relevance of each one; efficient knockdown of each channel with siRNAs was verified with no effect on the expression of the other channel partners (Figure 8D). TRPC1 and -6 knockdown did not have a significant effect on OAG- and Ang II-induced Ca^{2+} entries or cell proliferation (Figure 8, E–G). Because TRPC3 inhibition was sufficient to block Ca^{2+} entry with marked cellular effects, the roles of TRPC1 and -6 were not further studied; however, we could not exclude other cellular functions that might be accomplished by these channels.

TRPC3 Blockade Inhibits *In Vivo* Upregulation of TRPC3, ERK Activation, and High Proliferation Rate of Obstructed Kidneys Fibroblasts

Renal fibroblasts isolated from obstructed DMSO-treated kidneys showed relatively high expression of TRPC3 protein compared with sham renal fibroblasts (Figure 9, A and B). Increased TRPC3 expression was associated with enhanced ERK1/2 phosphorylation and correlated with high proliferation rates, which was shown by high levels of cell cycle regulators Ki67 and PCNA (Figure 9, A–C). TRPC3 blockade by pyr3 halted the increase in TRPC3 expression as well as ERK1/2 phosphorylation and cell proliferation (Figure 9, A and B).

TRPC3 Inhibition Reduced *In Vivo* Fibroblast Activation and ECM Remodeling

High TRPC3-mediated Ca^{2+} influx was recorded from obstructed kidneys fibroblasts under OAG stimulation (Figure 10A), whereas cells isolated from pyr3-treated kidneys showed marked decreases in Ca^{2+} influx (Figure 10A). Obstructed kidneys' myofibroblast contents decreased with TRPC3 blockade, which was shown by the diminished α-SMA expression (Figure 10B). The fibrotic and inflammatory activities of obstructed kidneys fibroblasts were drastically reduced under pyr3 treatment, and decreases were noted in fibroblast activation protein, TGF-β1, connective tissue growth factor, IL-1, IL-6, MCP1, cyclooxygenase 2, and arachidonate 5-lipoxygenase expressions compared with DMSO-treated kidneys (Figure 10C). ECM remodeling was also inhibited with TRPC3 blockade and led to significant decreases in total renal tissue collagen content (Figure 10D) as well as Fn, MMP2, MMP9, and TIMP1 proteins compared with DMSO-treated kidneys (Figure 10E).

TRPC3 Inhibition Ameliorates Fibrosis and Inflammation of the Obstructed Kidney

Semiquantitative analysis of renal sections stained with hematoxylin-eosin revealed that the obstructed kidneys treated by the vehicle developed severe tubulointerstitial damage with tubular atrophy and widened interstitial space with a greater number of interstitial cells and infiltrating leukocytes (Figure 11, C, D, and G–I) compared with sham kidneys (Figure, A, B, H, and I). These changes were observed in the whole cortex, although the degree of severity was not homogeneously distributed; pyr3 treatment markedly ameliorated these histologic alterations, with significant decreases in the scores of interstitial volume and the number of infiltrating leukocytes (Figure 11, E, F, H, and I).

The severity of renal fibrosis was assessed by Masson's trichrome total collagen staining. Increases in Masson's trichrome-positive areas showed marked interstitial fibrosis in the DMSO-treated UUO kidneys (Figure 12, C, D, and G) compared with sham kidneys (Figure 12, A, B, and G). TRPC3 blockade significantly decreased fibrotic area extensions (Figure 12, E–G).

TRPC3$^{-/-}$ Mice Exhibit Decreased Renal Fibroblast Activation and Are Protected Against Renal Fibrosis Induced by UUO

TRPC3$^{-/-}$ mice were previously developed and characterized.[70] After 10 days of UUO, mice kidneys were excised, and fibroblasts were isolated. Obstructed kidneys of TRPC3$^{-/-}$ mice showed relatively preserved renal parenchyma with fewer yellowish scars (Figure 13A). Compared with wild-type (WT) animals, UUO TRPC3$^{-/-}$ renal fibroblasts showed decreased levels of proliferation and differentiation as well as fibrotic and inflammatory markers (Figure 13B), which was in parallel to the reduction in ERK phosphorylation (Figure 13, C and D). Fibroblasts of sham TRPC3$^{-/-}$ mice presented comparable levels of the different studied markers as the WT animals (Figure 13, B–D).

Histopathology analysis revealed that renal tissue of TRPC3$^{-/-}$ mice was relatively preserved compared with WT mice, with much less tubulointerstitial damage, less tubular atrophy, less widened interstitial space, and a smaller number of interstitial cells and infiltrating leukocytes (Figure 14, A–D, I, and J). ECM accumulation stained with picrosirius red was much smaller than WT (Figure 14, E–H and K).

Upregulation of TRPC3 in the Interstitium of the Rat and Mouse Obstructed Kidneys

The observed renal tissue damage with the extensive fibrotic areas was accompanied by elevations in the interstitial α-SMA and TRPC3 expressions. In fact, sham rats and mice presented low interstitial α-SMA expression with some distribution around the blood vessels, whereas UUO drastically increased this α-SMA expression in the interstitium; pyr3-treated rats and TRPC3$^{-/-}$ mice exhibited significantly lower levels of this differentiation marker (Figure 15, A–F).

TRPC3 was widely distributed within the normal rat and mouse kidneys, and the expression was localized to the tubules, glomeruli, and interstitial cells (Figure 15, G and I). UUO caused a clear prominent upregulation of TRPC3 in the interstitium (Figure 15, I, K, and L). The interstitial distribution of TRPC3 was comparable with α-SMA. The specificity of the used anti-TRPC3 was confirmed on the TRPC3$^{-/-}$ kidney sections, which did not show any labeling, even after UUO (Figure 15, H and J).

Discussion

Renal fibrosis is a result of most acute kidney diseases as well as CKD, with fibroblasts proliferation and differentiation into myofibroblasts being its most important key player.[71] UUO is a well established model of renal fibrosis that allows the study of different pathologic aspects, such as EMT, tubular atrophy, inflammation, and interstitial fibrosis, in a relatively short time. Nonselective Ca^{2+} permeant TRPC channels (more specifically, TRPC3) have been implicated in many cardiorenal diseases, such as cardiac hypertrophy[36–39,42] and hypertension.[28,31,33–35] Some studies showed a certain correlation with kidney disease.[27,32,50] However, no study to our knowledge has investigated the role of fibroblast TRPC3 in renal disease, such as fibrosis, and whether its inhibition could prevent the development of renal dysfunction. In this work, we sought to study TRPC3 as a potential target in treating and preventing renal fibrosis.

Isolated renal fibroblasts showed a strong expression of functional TRPC3, with large Ca^{2+} entries observed after stimulation with OAG. Furthermore, pyr3, a selective inhibitor of this channel, showed dose-dependent inhibition of OAG-induced Ca^{2+} entry in these cells, with marked effects in either acute or chronic (preincubation) inhibition; pyr3 has been shown to possess specific inhibitory effects on TRPC3 without any action on the other TRPC isoforms (TRPC1, -2, -4, -5, -6, and -7) as well as melastatin-related transient receptor potential TRPM2, -4, and -7.[42] The action site of pyr3 is located on the external side of the TRPC3 protein, and similar acute actions of pyr3 were noted in human coronary artery smooth muscle cells and microvascular endothelial cells.[42,43] DAG analog OAG has been routinely used as a direct activator of receptor operated channels TRPC3 and -6 independently of protein kinases C and without the generation of inositol trisphosphate.[59] Nonselective blockers SKF96365, Gd^{3+}, and 2-APB were also used to further validate the implication of TRP channels. Recently, the presence of TRPC channels has been depicted in a normal rat kidney fibroblasts cell line and found to control the process of receptor-operated Ca^{2+} influx[46,47]; additionally, TRPC3 was present in the rat kidney and played a key role in the influx of Ca^{2+} into principal cells of the collecting duct.[48,52–54] However, the role of such channels in freshly isolated adult renal fibroblasts under native physiologic conditions remains to be elucidated.

The renin-angiotensin system is also known to play a key role in the progression of chronic kidney damage contributing to renal fibrosis. UUO is associated with increased plasma Ang II that activates renal cells to produce profibrotic factors and ECM,[72–77] and TRPC3 has been shown to be activated among others by Ang II.[78,79] Hence, we assessed the role of TRPC3 in Ang II-mediated Ca^{2+} entry in renal fibroblasts and found that pyr3 drastically affected Ang II response. The above-observed Ca^{2+} entries were stimulated by either OAG or Ang II; hence, we checked for a possible basal constitutive Ca^{2+} entry. However, on and off switching of the extracellular Ca^{2+} did not result in a significant Ca^{2+} entry.

The Mn^{2+} quench technique was also used to estimate the sarcolemmal permeability to divalent cations. Mn^{2+}, as a surrogate for Ca^{2+}, enters cells through the same routes as Ca^{2+} and accumulates inside over time, because it is poorly accepted by the cellular transport systems. Mn^{2+} irreversibly quenches fura-2 fluorescence, and the reduction of the intensity of fura-2 fluorescence can be used as an indicator of the time integral of Mn^{2+} influx.[80,81] The experiments with Mn^{2+} confirmed the previous results as to the functional relevance of TRPC3 in renal fibroblasts.

Ca^{2+} is a universal second messenger that plays important roles in proliferation and transcription.[22] Similar

to dose-dependent inhibition of OAG/Ang II-induced Ca^{2+} entries by pyr3, TRPC3 blockade inhibited *in vitro* renal fibroblast proliferation in a dose-dependent manner with upregulation of negative cell cycle regulators. This antiproliferative effect of TRPC3 blockade was shown on cardiac fibroblasts.[44] TRPC3-mediated Ca^{2+} influx may trigger downstream activation of signaling pathways leading to fibroblast proliferation. Indeed, recent reports showed TRPC3 association with ERK pathway activation.[44,82] However, Ang II induced proliferation of cardiac fibroblasts through ERK1/2 cascade.[83–85] This prompted us to evaluate the activation of the ERK pathway in renal fibroblasts and its dependence on TRPC3; TRPC3 blockade resulted in ERK1/2 phosphorylation inhibition, which was further validated by selective ERK1/2 inhibition resulting in decreased cell proliferation. TRPC3-mediated activation of ERK1/2 was dependent on Ca^{2+}, because extracellular omission of this ion diminished ERK1/2 phosphorylation and fibroblast proliferation.

Myofibroblasts play a crucial role in the pathophysiology of fibrosis by possessing an active secretory phenotype; these cells synthesize ECM components and have the defining feature of forming α-SMA stress fibers.[11,86] The role of TRPC3 in fibroblast to myofibroblast differentiation was investigated. TRPC3 inhibition led to decreases in α-SMA expression as well as profibrotic and inflammatory cytokines; this effect was dependent on ERK1/2 activation, because selective blockade of this pathway resulted in diminished collagen and IL synthesis. Studies showed that adenoviral overexpression of TRPC3 induced significant differentiation of fibroblasts into myofibroblasts,[87] whereas Ca^{2+} and ERK1/2 pathways were essential in ECM collagen synthesis and cytokines production.[88–91] The observed effects of TRPC3 inhibition were mediated in a noncytotoxic manner.

TRPC3-specific knockdown confirmed the pharmacologic findings; diminished OAG and Ang II-induced Ca^{2+} entries were observed with siTRPC3 as well as decreased renal fibroblast proliferation. TRPC3 knockdown inhibited the phenotype switch to myofibroblasts, which was dependent on ERK1/2 phosphorylation. The activated myofibroblastic fibrotic and inflammatory phenotype was also abolished with TRPC3 knockdown.

TRPC channels were shown to assemble in heteromultimers; more specifically, TRPC3, -6, and -7 form a structural and functional TRPC subfamily characterized by their sensitivity toward DAG.[59,92–97] TRPC3 and -6 may also compensate for the loss of one or the other in knockout strategies, which was previously shown in $TRPC6^{-/-}$ mice.[95] These mice exhibited increased BP and higher basal cation entry caused by the upregulation of TRPC3. One could speculate that pyr3 administration might abolish and reverse the observed effects in these mice. Furthermore, fibroblasts contain several TRPC channel subtypes, such as TRPC3 and -6,[44,87] whereas kidneys contained TRPC1, -3, and -6.[48] Therefore, we characterized the expression and functional relevance of TRPC isoforms in our studied cells. TRPC1, -3, and -6 were found at the mRNA and protein levels and assembled together, whereas the other isoforms were not detectable. Specific siRNA-mediated TRPC1 and -6 knockdown did not affect Ca^{2+} entries and cell proliferation. Likewise, previous studies showed that TRPC1 did not form functional homomeric channels,[98] whereas TRPC6 was absent in fibroblasts.[87] Consequently, because TRPC3 inhibition was sufficient in blocking Ca^{2+} entries, we did not further investigate the roles of these channels in renal fibroblasts function. However, we could not exclude a possible role of these channels in other Ca^{2+} entries and cellular functions.

In our UUO model of kidney disease, TRPC3 expression increased in renal fibroblasts of obstructed kidneys, with parallel increases in OAG-induced Ca^{2+} influx and cell proliferation. This might be because of a positive feed-forward regulation of TRPC3; in fact, this positive feed-forward regulation of TRPC signaling was reported for excessive TRPC activation in other cell types.[43,99] During tissue injuries, such as those occurring in kidney diseases, mesenchymal and inflammatory cells secrete a wide array of profibrotic and inflammatory cytokines, such as TGF-β1, Ang II, and endothelin I, contributing to the differentiation of

fibroblasts into myofibroblasts.[71,86] Furthermore, the ERK signaling pathway is activated in UUO and may provide approaches in preventing progression of renal fibrosis.[100,101] As expected, α-SMA expression as well as ERK1/2 phosphorylation, renal fibroblasts proliferation, and activation increased in obstructed kidneys. *In vivo*, TRPC3 inhibition abrogated these changes, pointing toward an important role of TRPC3 in the pathogenesis of kidney disease simulated by the UUO model. Then, we evaluated the effect of TRPC3 inhibition on the prevention of ECM remodeling and renal fibrosis. Net decreases in collagen, MMP2/9, and TIMP1 were noted with TRPC3 inhibition. UUO also caused leukocyte infiltration of the kidney and severe tubulointerstitial fibrosis with widened interstitial space. These histologic changes were remarkably improved with TRPC3 blockade.

The importance of TRPC3 in the development of renal fibrosis was further promoted by the use of TRPC3$^{-/-}$ mice. Similar to the rat model, UUO induced the upregulation of TRPC3 and the activation of ERK pathway in the renal fibroblasts of WT mice. However, TRPC3$^{-/-}$ mice did not show this pronounced ERK activation and were protected against renal damage and fibrosis. Noteworthy was the distribution of TRPC3 in the rat and mouse renal tissues. In fact, TRPC3 was localized in the glomeruli, tubules, and interstitium, and this expression was only increased in the interstitial cells. TRPC channels, specifically TRPC1, -3, and -6, were previously identified and localized in the glomeruli and tubules of the adult rat kidney, but the interstitial localization was not investigated.[48]

This study was conducted on TRPC3 in renal fibroblasts to evaluate its implication in the development of renal fibrosis. However, this could not eliminate a possible role of TRPC3 in other cell types, such as monocytes, in the fibrogenic process; monocytes were implicated in hypertension and inflammation through a TRPC3 pathway.[28,29,33,35]

In conclusion, this work showed, for the first time, the presence and the functional role of TRPC3-mediated Ca^{2+} influx and ERK cascade signaling in renal fibroblasts under pathologic conditions. TRPC3 inhibition and its knockout prevented renal damage and fibrosis associated with UUO. TRPC3 could be a new candidate for better understanding the pathophysiology of renal fibrogenesis as well as a new potential pharmacologic target in treating renal fibrosis.

Concise Methods

Additional details are in Supplemental Material.

Animals

The protocols of this study were designed according to the Guiding Principles in the Care and Use of Animals approved by the Council of the American Physiologic Society and were in adherence to the Guide for the Care and Use of Laboratory Animals by the US National Institutes of Health. The study was conducted in adult male Wistar rats (220±20 g) and male 8- to 10-week-old TRPC3$^{-/-}$ mice with their age-matched littermate WT controls. Rats were obtained from the Centre d'Elevage R. Janvier (Le Genest-Saint Isle, France), whereas mice were developed at the laboratory of L.B. at the National Institute of Environmental Health Sciences as previously described[70] and obtained from the laboratory stock of Nancy Rusch at the University of Arkansas for Medical Sciences.

Generation of TRPC3$^{-/-}$ Mice

TRPC3$^{-/-}$ mice were generated by disrupting the *Trpc3* gene in a three-step process as previously described.[70]

Fibroblast Isolation and Culture

Primary renal fibroblast cultures were prepared as previously described with some modifications.[102–107] Briefly, animals were anesthetized with ketamine (75 mg/kg; Interchemie, Waalre, Holland) and xylazine (10 mg/kg; RotexMedica, Trittau, Germany). Kidneys were harvested and rinsed with cold tyrode solution with the following composition: 117 mM NaCl, 5.7 mM KCl, 1.7 mM $MgCl_2$, 4.4 mM $NaHCO_3$, 1.5 mM KH_2PO_4, 10 mM Hepes, 10 mM creatinine monohydrate, 20 mM taurine, 11.7 mM D-glucose, and 1% BSA (pH 7.1) with NaOH. Kidneys were then digested by two oxygenated enzymatic baths (90 rpm shaker at 37°C) for 1 hour. The baths contained 1 $mg{\cdot}ml^{-1}$ collagenase A (Roche Diagnostics) with 1 $mg{\cdot}ml^{-1}$ BSA (Sigma-Aldrich, St. Louis, MO). Renal tubules were discarded after the first centrifugation (500 rpm for 10 minutes), and then, the remaining cells were collected after the second centrifugation (2000 rpm for 10 minutes). These remaining cells were put onto a Percoll gradient consisting of four different concentrations (40%, 20%, 10%, and 5%) and centrifuged at 500 rpm for 20 minutes. The cell layers obtained in the interface between the 5% and 10% Percoll were collected and resuspended in DMEM containing 10% FBS (Lonza, Basel, Switzerland) and 1% penicillin/streptomycin.

Cell Culture Treatments

Renal fibroblasts were kept in culture for 3 days before treatment by the pyrazole-derivative TRPC3 blocker pyr3 (Tocris Bioscience, Bristol, UK) diluted in 100% DMSO for 2 days (10 μM) as previously described.[40–43] When ERK inhibitors were used, cells were treated after 3 days of culture for 24 hours with 50 μM PD98059 or 10 μM U0126 (Tocris Bioscience). Sixteen cultures from eight rats were performed for each condition.

Ca^{2+} Imaging

Cultured renal fibroblasts grown for 3 days on glass coverslips were incubated for 45 minutes in serum free DMEM containing 4 μM fura2-am (Molecular Probes; Life Technologies, Carlsbad, CA). Cells were washed two times in standard Hepes-buffered saline solution containing 135 mM NaCl, 4 mM KCl, 1.8 mM $CaCl_2$, 1 mM $MgCl_2$, 2.5 mM Hepes, and 10 mM glucose (pH 7.4) with NaOH. Perfusion protocols were performed using either DAG analog OAG (100 μM) or Ang II (100 nM; Sigma-Aldrich). Nifedipine (1 μM) was used to inhibit the previously reported L-type Ca^{2+} channels[108–111]; pyr3 was added at a concentration of 10 μM. The nonselective TRPC channel blockers SKF96365 (30 μM), gadolinium Gd^{3+} (100 μM), and 2-APB (75 μM) were from Sigma-Aldrich. Ionomycin (2 μM) and EGTA (10 mM) were consecutively added at the end of the perfusion protocols to check for the maximum and minimum fluorescence values. When Ca^{2+} imaging on siRNA-transfected cultures was performed, either transfected cells (tagged cy3-siTRPC1, -3, and -6) or nontransfected cells were analyzed after 48 hours of transfection. Freshly isolated fibroblasts from sham and UUO kidneys were incubated for 12 hours on glass coverslips before performing Ca^{2+} recordings. Intracellular Ca^{2+} concentration was estimated as described by Grynkiewicz *et al*.[112]

Fluorescence quenching experiments were carried out by the addition of 50 μM $MnCl_2$ to the Hepes-buffered saline solution medium. Fluorescent measurements were performed at the isosbestic point of fura-2 (360 nm). The manganese influx was quantified by the slope of the quenching kinetics. Emitted fura fluorescence was collected through a 510-nm filter. The calcium and contractility recording system (IonOptix) was used. Data analysis was performed using the ionwizard software (version 6.1) and sigmaPlot (version 11.0). Data are represented as means±SEMs.

Cell Proliferation and Viability

Cell proliferation assay was done using MTT (Bio Basic Inc., Markham, ON, Canada). Cell viability was assessed by the Trypan blue exclusion test. H_2O_2 was used on cells at a concentration of 1 mM for 4 hours

at 37°C as a positive control to induce cell mortality.[113,114]

Sircol Collagen Assay

Collagen synthesis by cultured fibroblasts as well as collagen dosage from tissue of sham and obstructed kidneys were evaluated by the sircol collagen assay (Biocolor, County Antrim, UK) as described in the manufacturer technical sheet.

Cell Transfection

Cells were transfected with cy3-tagged siRNAs on day 3 and left for 48 hours before assessing TRPC1, -3, and -6 knockout effects. The turbofect transfection reagent (Thermo Fisher Scientific) was used according to the manufacturer protocol. siRNA sequences were from Eurogentec (Seraing, Belgium): cy3-siTRPC1: sense, 5′-CUGCUCAUCGUAACAACUA-3′ and antisense, 5′-UAGUUGUUACGAUGAGCAG-3′; cy3-siTRPC3: sense, 5′-CAUUCUCAAUCAGCCAACACGAUAU-3′ and antisense, 5′-AUAUCGUGUUGGCUGAUUGAGAAUG-3′; cy3-siTRPC6: sense, 5′-GGACCAGCAUACAUGUUUA-3′ and antisense, 5′-UAAACAUGUAUGCUGGUCC -3′; and cy3-siScrambled: sense, 5′-AAUACUCGCCCUAAUCCACAGAUAU-3′ and antisense, 5′-AUAUCUGUGGAUUAGGGCGAGUAUU-3′.

Coimmunoprecipitation and Western Blot

Total proteins were extracted from both cultured or freshly isolated renal fibroblasts and renal tissue from rats and mice. To perform immunoprecipitations, 500 μg protein was incubated overnight at 4°C in the presence of anti-TRPC1 (20 μg), anti-TRPC3 (20 μg), anti-TRPC6 (20 μg), or a nonrelevant antibody (rabbit IgG) used as a negative control. Prewashed A/G agarose beads were then added, proteins were eluted and separated by 10% SDS-PAGE, and then, they were blotted on Hybond-C membranes (Amersham Biosciences; GE Healthcare). Membranes were incubated with anti-TRPC1 (1/200), anti-TRPC3 (1/200), and anti-TRPC6 (1/200). The remaining Western blots were with the following primary antibodies: anti-p53 (1/500), anti-p21 (1/500), anti-PCNA (1/1000), anti-Ki67 (1/1000), α-SMA (1/1000), total ERK1/2 (1/1000), phospho-ERK (1/500), Fn (1/1000), MMP2 (1/1000), MMP9 (1/1000), and TIMP1 (1/500; Abcam, Inc.).

ELISA

The ELISA technique was used for quantifying secreted cytokines from cell cultures. TGF-β1, IL-1, and IL-6 rat ELISA kits were used according to the manufacturer protocols (Abcam, Inc.).

Immunocytochemistry

Renal fibroblasts were grown on glass slides for either 12 hours (day 0 staining) or 5 days (day 5 staining) and fixed with 100% ice-cold ethanol. Primary antibodies were antivimentin (1/250) and anticytokeratin (1/250; Abcam, Inc.).

UUO

Under adequate anesthesia, the left ureter was ligated with 4–0 silk at two points. Rats were divided in three groups of 10 rats each: UUO-DMSO, where animals underwent UUO and were treated with DMSO and polyethylene glycol; UUO-pyr3, where animals underwent UUO and were treated with pyr3 (0.1 mg/kg per day[42]); and sham, where animals were also treated with the same dose of pyr3. Osmotic pumps were implanted subcutaneously in the back 3 days before UUO and kept until euthanasia at day 10.

Similarly, UUO was conducted on mice; animals were divided in four groups of eight mice each: UUO-

WT, UUO-TRPC3$^{-/-}$, sham WT, and sham TRPC3$^{-/-}$.

Renal Tissue Preparation for Histopathology

Left kidneys from both rats and mice were excised, decapsulated, and then cut in half through a midsagittal plane. One half was fixed with 10% formalin solution (Sigma-Aldrich), whereas the other one half was dissected into three pieces destined for fibroblast cell isolation as well as RNA and protein extractions. The formalin-fixed tissue was embedded in paraffin, and sections of 4-μm thickness were cut. Paraffin-embedded sections of the kidneys were stained with hematoxylin-eosin and Masson's trichrome (Sigma-Aldrich). Mice kidneys were further stained with picrosirius red (Sigma-Aldrich) as well as α-SMA (BioGenex) and TRPC3 (Abcam, Inc.) antibodies.

Gene Quantifications

Total RNA was extracted from the previously treated cultured renal fibroblasts as well as the freshly isolated cells from sham and UUO kidneys (rats and mice) by the use of Trizol (Life Technologies). cDNA was synthesized using the Superscript III Reverse Transcription Kit (Life Technologies). Real-time PCR was conducted using the 7500 Real-Time PCR System and the Sybr Green PCR Master Mix (Life Technologies). The primers (Eurogentec) used are presented in Supplemental Table 1.

Statistical Analyses

All quantitative data are reported as means±SEMs. Statistical analysis was performed with the SigmaPlot (version 11.0) software. One-way ANOVA tests were performed for multiple comparisons of values. *Post hoc* two-tailed *t* test comparisons were performed to identify which group differences accounted for significant overall ANOVA results. All values with $P<0.05$ were considered significant.

Disclosures

None.

Supplementary Material

Supplemental Data:

Acknowledgments

We thank Nancy Rusch at the University of Arkansas for Medical Sciences for providing the TRPC3$^{-/-}$ mice.

This work was supported by the Research Council of the Saint Joseph University Faculty of Medicine and in part by Intramural Research Program of the US National Institutes of Health Project Z01-ES-101684 (to L.B.).

Footnotes

Published online ahead of print. Publication date available at www.jasn.org.

This article contains supplemental material online at http://jasn.asnjournals.org/lookup/suppl/doi:10.1681/ASN.2014010065/-/DCSupplemental.

References

1. Coresh J, Selvin E, Stevens LA, Manzi J, Kusek JW, Eggers P, Van Lente F, Levey AS: Prevalence of

chronic kidney disease in the United States. JAMA 298: 2038–2047, 2007 [PubMed: 17986697]

2. Coresh J, Stevens LA, Levey AS: Chronic kidney disease is common: What do we do next? Nephrol Dial Transplant 23: 1122–1125, 2008 [PubMed: 18359871]

3. Becker GJ, Hewitson TD: The role of tubulointerstitial injury in chronic renal failure. Curr Opin Nephrol Hypertens 9: 133–138, 2000 [PubMed: 10757217]

4. Boor P, Ostendorf T, Floege J: Renal fibrosis: Novel insights into mechanisms and therapeutic targets. Nat Rev Nephrol 6: 643–656, 2010 [PubMed: 20838416]

5. Gagliardini E, Benigni A: Therapeutic potential of TGF-beta inhibition in chronic renal failure. Expert Opin Biol Ther 7: 293–304, 2007 [PubMed: 17309322]

6. Liu Y: Renal fibrosis: New insights into the pathogenesis and therapeutics. Kidney Int 69: 213–217, 2006 [PubMed: 16408108]

7. Zeisberg M, Neilson EG: Mechanisms of tubulointerstitial fibrosis. J Am Soc Nephrol 21: 1819–1834, 2010 [PubMed: 20864689]

8. Wynn TA, Ramalingam TR: Mechanisms of fibrosis: Therapeutic translation for fibrotic disease. Nat Med 18: 1028–1040, 2012 [PMCID: PMC3405917] [PubMed: 22772564]

9. Liu Y: Epithelial to mesenchymal transition in renal fibrogenesis: Pathologic significance, molecular mechanism, and therapeutic intervention. J Am Soc Nephrol 15: 1–12, 2004 [PubMed: 14694152]

10. Neilson EG: Mechanisms of disease: Fibroblasts—a new look at an old problem. Nat Clin Pract Nephrol 2: 101–108, 2006 [PubMed: 16932401]

11. Wynn TA: Cellular and molecular mechanisms of fibrosis. J Pathol 214: 199–210, 2008 [PMCID: PMC2693329] [PubMed: 18161745]

12. Schlondorff DO: Overview of factors contributing to the pathophysiology of progressive renal disease. Kidney Int 74: 860–866, 2008 [PubMed: 18650795]

13. Humphreys BD, Lin SL, Kobayashi A, Hudson TE, Nowlin BT, Bonventre JV, Valerius MT, McMahon AP, Duffield JS: Fate tracing reveals the pericyte and not epithelial origin of myofibroblasts in kidney fibrosis. Am J Pathol 176: 85–97, 2010 [PMCID: PMC2797872] [PubMed: 20008127]

14. Lin SL, Kisseleva T, Brenner DA, Duffield JS: Pericytes and perivascular fibroblasts are the primary source of collagen-producing cells in obstructive fibrosis of the kidney. Am J Pathol 173: 1617–1627, 2008 [PMCID: PMC2626374] [PubMed: 19008372]

15. Kriz W, Kaissling B, Le Hir M: Epithelial-mesenchymal transition (EMT) in kidney fibrosis: Fact or fantasy? J Clin Invest 121: 468–474, 2011 [PMCID: PMC3026733] [PubMed: 21370523]

16. Zavadil J, Haley J, Kalluri R, Muthuswamy SK, Thompson E: Epithelial-mesenchymal transition. Cancer Res 68: 9574–9577, 2008 [PubMed: 19047131]

17. Zeisberg EM, Tarnavski O, Zeisberg M, Dorfman AL, McMullen JR, Gustafsson E, Chandraker A, Yuan X, Pu WT, Roberts AB, Neilson EG, Sayegh MH, Izumo S, Kalluri R: Endothelial-to-mesenchymal transition contributes to cardiac fibrosis. Nat Med 13: 952–961, 2007 [PubMed: 17660828]

18. Zeisberg EM, Potenta SE, Sugimoto H, Zeisberg M, Kalluri R: Fibroblasts in kidney fibrosis emerge via endothelial-to-mesenchymal transition. J Am Soc Nephrol 19: 2282–2287, 2008 [PMCID: PMC2588112] [PubMed: 18987304]

19. Zeisberg EM, Potenta S, Xie L, Zeisberg M, Kalluri R: Discovery of endothelial to mesenchymal transition as a source for carcinoma-associated fibroblasts. Cancer Res 67: 10123–10128, 2007 [PubMed: 17974953]

20. Zeisberg M, Duffield JS: Resolved: EMT produces fibroblasts in the kidney. J Am Soc Nephrol 21: 1247–1253, 2010 [PubMed: 20651165]

21. Berridge MJ: Calcium signalling remodelling and disease. Biochem Soc Trans 40: 297–309, 2012 [PubMed: 22435804]

22. Berridge MJ, Bootman MD, Roderick HL: Calcium signalling: Dynamics, homeostasis and remodelling. Nat Rev Mol Cell Biol 4: 517–529, 2003 [PubMed: 12838335]

23. Yue L, Xie J, Nattel S: Molecular determinants of cardiac fibroblast electrical function and therapeutic implications for atrial fibrillation. Cardiovasc Res 89: 744–753, 2011 [PMCID: PMC3039247] [PubMed: 20962103]

24. Clapham DE: TRP channels as cellular sensors. Nature 426: 517–524, 2003 [PubMed: 14654832]

25. Hallam TJ, Rink TJ: Agonists stimulate divalent cation channels in the plasma membrane of human platelets. FEBS Lett 186: 175–179, 1985 [PubMed: 2408921]

26. Horinouchi T, Terada K, Higa T, Aoyagi H, Nishiya T, Suzuki H, Miwa S: Function and regulation of endothelin type A receptor-operated transient receptor potential canonical channels. J Pharmacol Sci 117: 295–306, 2011 [PubMed: 22129540]

27. Liu Y, Thilo F, Kreutz R, Schulz A, Wendt N, Loddenkemper C, Jankowski V, Tepel M: Tissue expression of TRPC3 and TRPC6 in hypertensive Munich Wistar Frömter rats showing proteinuria. Am J Nephrol 31: 36–44, 2010 [PubMed: 19887786]

28. Liu D, Scholze A, Zhu Z, Kreutz R, Wehland-von-Trebra M, Zidek W, Tepel M: Increased transient receptor potential channel TRPC3 expression in spontaneously hypertensive rats. Am J Hypertens 18: 1503–1507, 2005 [PubMed: 16280289]

29. Thilo F, Scholze A, Liu DY, Zidek W, Tepel M: Association of transient receptor potential canonical type 3 (TRPC3) channel transcripts with proinflammatory cytokines. Arch Biochem Biophys 471: 57–62, 2008 [PubMed: 18177730]

30. Thilo F, Baumunk D, Krause H, Schrader M, Miller K, Loddenkemper C, Zakrzewicz A, Krueger K, Zidek W, Tepel M: Transient receptor potential canonical type 3 channels and blood pressure in humans. J Hypertens 27: 1217–1223, 2009 [PubMed: 19417689]

31. Thilo F, Loddenkemper C, Berg E, Zidek W, Tepel M: Increased TRPC3 expression in vascular endothelium of patients with malignant hypertension. Mod Pathol 22: 426–430, 2009 [PubMed: 19136933]

32. Liu Y, Krueger K, Hovsepian A, Tepel M, Thilo F: Calcium-dependent expression of transient receptor potential canonical type 3 channels in patients with chronic kidney disease. Arch Biochem Biophys 514: 44–49, 2011 [PubMed: 21802402]

33. Wang P, Liu D, Tepel M, Zhu Z: Transient receptor potential canonical type 3 channels—their evolving role in hypertension and its related complications. J Cardiovasc Pharmacol 61: 455–460, 2013 [PubMed: 23364606]

34. Adebiyi A, Thomas-Gatewood CM, Leo MD, Kidd MW, Neeb ZP, Jaggar JH: An elevation in physical coupling of type 1 inositol 1,4,5-trisphosphate (IP3) receptors to transient receptor potential 3 (TRPC3) channels constricts mesenteric arteries in genetic hypertension. Hypertension 60: 1213–1219, 2012

[PMCID: PMC3632264] [PubMed: 23045459]

35. Zhao Z, Ni Y, Chen J, Zhong J, Yu H, Xu X, He H, Yan Z, Scholze A, Liu D, Zhu Z, Tepel M: Increased migration of monocytes in essential hypertension is associated with increased transient receptor potential channel canonical type 3 channels. PLoS ONE 7: e32628, 2012 [PMCID: PMC3306381] [PubMed: 22438881]

36. Wu X, Eder P, Chang B, Molkentin JD: TRPC channels are necessary mediators of pathologic cardiac hypertrophy. Proc Natl Acad Sci U S A 107: 7000–7005, 2010 [PMCID: PMC2872458] [PubMed: 20351294]

37. Nakayama H, Wilkin BJ, Bodi I, Molkentin JD: Calcineurin-dependent cardiomyopathy is activated by TRPC in the adult mouse heart. FASEB J 20: 1660–1670, 2006 [PMCID: PMC2693319] [PubMed: 16873889]

38. Bush EW, Hood DB, Papst PJ, Chapo JA, Minobe W, Bristow MR, Olson EN, McKinsey TA: Canonical transient receptor potential channels promote cardiomyocyte hypertrophy through activation of calcineurin signaling. J Biol Chem 281: 33487–33496, 2006 [PubMed: 16950785]

39. Brenner JS, Dolmetsch RE: TrpC3 regulates hypertrophy-associated gene expression without affecting myocyte beating or cell size. PLoS ONE 2: e802, 2007 [PMCID: PMC1950081] [PubMed: 17726532]

40. Sabourin J, Robin E, Raddatz E: A key role of TRPC channels in the regulation of electromechanical activity of the developing heart. Cardiovasc Res 92: 226–236, 2011 [PubMed: 21672930]

41. Sabourin J, Antigny F, Robin E, Frieden M, Raddatz E: Activation of transient receptor potential canonical 3 (TRPC3)-mediated Ca2+ entry by A1 adenosine receptor in cardiomyocytes disturbs atrioventricular conduction. J Biol Chem 287: 26688–26701, 2012 [PMCID: PMC3411008] [PubMed: 22692208]

42. Kiyonaka S, Kato K, Nishida M, Mio K, Numaga T, Sawaguchi Y, Yoshida T, Wakamori M, Mori E, Numata T, Ishii M, Takemoto H, Ojida A, Watanabe K, Uemura A, Kurose H, Morii T, Kobayashi T, Sato Y, Sato C, Hamachi I, Mori Y: Selective and direct inhibition of TRPC3 channels underlies biological activities of a pyrazole compound. Proc Natl Acad Sci U S A 106: 5400–5405, 2009 [PMCID: PMC2664023] [PubMed: 19289841]

43. Koenig S, Schernthaner M, Maechler H, Kappe CO, Glasnov TN, Hoefler G, Braune M, Wittchow E, Groschner K: A TRPC3 blocker, ethyl-1-(4-(2,3,3-trichloroacrylamide)phenyl)-5-(trifluoromethyl)-^{1}H-pyrazole-4-carboxylate (Pyr3), prevents stent-induced arterial remodeling. J Pharmacol Exp Ther 344: 33–40, 2013 [PubMed: 23010361]

44. Harada M, Luo X, Qi XY, Tadevosyan A, Maguy A, Ordog B, Ledoux J, Kato T, Naud P, Voigt N, Shi Y, Kamiya K, Murohara T, Kodama I, Tardif JC, Schotten U, Van Wagoner DR, Dobrev D, Nattel S: Transient receptor potential canonical-3 channel-dependent fibroblast regulation in atrial fibrillation. Circulation 126: 2051–2064, 2012 [PMCID: PMC3675169] [PubMed: 22992321]

45. Ikeda K, Nakajima T, Yamamoto Y, Takano N, Tanaka T, Kikuchi H, Oguri G, Morita T, Nakamura F, Komuro I: Roles of transient receptor potential canonical (TRPC) channels and reverse-mode Na+/Ca2+ exchanger on cell proliferation in human cardiac fibroblasts: Effects of transforming growth factor β1. Cell Calcium 54: 213–225, 2013 [PubMed: 23827314]

46. Almirza WH, Peters PH, van Zoelen EJ, Theuvenet AP: Role of Trpc channels, Stim1 and Orai1 in PGF(2α)-induced calcium signaling in NRK fibroblasts. Cell Calcium 51: 12–21, 2012 [PubMed: 22050845]

47. Dernison MM, Almirza WH, Kusters JM, van Meerwijk WP, Gielen CC, van Zoelen EJ, Theuvenet AP: Growth-dependent modulation of capacitative calcium entry in normal rat kidney fibroblasts. Cell Signal 22: 1044–1053, 2010 [PubMed: 20188167]

48. Goel M, Sinkins WG, Zuo CD, Estacion M, Schilling WP: Identification and localization of TRPC channels in the rat kidney. Am J Physiol Renal Physiol 290: F1241–F1252, 2006 [PubMed: 16303855]

49. Facemire CS, Mohler PJ, Arendshorst WJ: Expression and relative abundance of short transient receptor potential channels in the rat renal microcirculation. Am J Physiol Renal Physiol 286: F546–F551, 2004 [PubMed: 14678949]

50. Woudenberg-Vrenken TE, Bindels RJ, Hoenderop JG: The role of transient receptor potential channels in kidney disease. Nat Rev Nephrol 5: 441–449, 2009 [PubMed: 19546862]

51. Letavernier E, Rodenas A, Guerrot D, Haymann JP: Williams-Beuren syndrome hypercalcemia: Is TRPC3 a novel mediator in calcium homeostasis? Pediatrics 129: e1626–e1630, 2012 [PubMed: 22566418]

52. Goel M, Schilling WP: Role of TRPC3 channels in ATP-induced Ca2+ signaling in principal cells of the inner medullary collecting duct. Am J Physiol Renal Physiol 299: F225–F233, 2010 [PMCID: PMC2904168] [PubMed: 20410214]

53. Goel M, Zuo CD, Schilling WP: Role of cAMP/PKA signaling cascade in vasopressin-induced trafficking of TRPC3 channels in principal cells of the collecting duct. Am J Physiol Renal Physiol 298: F988–F996, 2010 [PMCID: PMC2853306] [PubMed: 20107112]

54. Goel M, Sinkins WG, Zuo CD, Hopfer U, Schilling WP: Vasopressin-induced membrane trafficking of TRPC3 and AQP2 channels in cells of the rat renal collecting duct. Am J Physiol Renal Physiol 293: F1476–F1488, 2007 [PubMed: 17699554]

55. Chevalier RL, Forbes MS, Thornhill BA: Ureteral obstruction as a model of renal interstitial fibrosis and obstructive nephropathy. Kidney Int 75: 1145–1152, 2009 [PubMed: 19340094]

56. Vaughan ED, Jr., Marion D, Poppas DP, Felsen D: Pathophysiology of unilateral ureteral obstruction: Studies from Charlottesville to New York. J Urol 172: 2563–2569, 2004 [PubMed: 15538209]

57. Klahr S, Morrissey J: Obstructive nephropathy and renal fibrosis. Am J Physiol Renal Physiol 283: F861–F875, 2002 [PubMed: 12372761]

58. Kim DH, Moon SO, Jung YJ, Lee AS, Kang KP, Lee TH, Lee S, Chai OH, Song CH, Jang KY, Sung MJ, Zhang X, Park SK, Kim W: Mast cells decrease renal fibrosis in unilateral ureteral obstruction. Kidney Int 75: 1031–1038, 2009 [PubMed: 19242503]

59. Hofmann T, Obukhov AG, Schaefer M, Harteneck C, Gudermann T, Schultz G: Direct activation of human TRPC6 and TRPC3 channels by diacylglycerol. Nature 397: 259–263, 1999 [PubMed: 9930701]

60. Venkatachalam K, Zheng F, Gill DL: Regulation of canonical transient receptor potential (TRPC) channel function by diacylglycerol and protein kinase C. J Biol Chem 278: 29031–29040, 2003 [PubMed: 12721302]

61. Bird GS, DeHaven WI, Smyth JT, Putney JW, Jr.: Methods for studying store-operated calcium entry. Methods 46: 204–212, 2008 [PMCID: PMC2643845] [PubMed: 18929662]

62. Anderson M: Mn ions pass through calcium channels. A possible explanation. J Gen Physiol 81: 805–827, 1983 [PMCID: PMC2215560] [PubMed: 6308126]

63. Scumpia PO, McAuliffe PF, O'Malley KA, Ungaro R, Uchida T, Matsumoto T, Remick DG, Clare-Salzler MJ, Moldawer LL, Efron PA: CD11c+ dendritic cells are required for survival in murine polymicrobial sepsis. J Immunol 175: 3282–3286, 2005 [PubMed: 16116220]

64. Krüger T, Benke D, Eitner F, Lang A, Wirtz M, Hamilton-Williams EE, Engel D, Giese B, Müller-Newen G, Floege J, Kurts C: Identification and functional characterization of dendritic cells in the healthy murine kidney and in experimental glomerulonephritis. J Am Soc Nephrol 15: 613–621, 2004 [PubMed: 14978163]

65. Whyte DA, Li C, Thomson RB, Nix SL, Zanjani R, Karp SL, Aronson PS, Igarashi P: Ksp-cadherin gene promoter. I. Characterization and renal epithelial cell-specific activity. Am J Physiol 277: F587–F598, 1999 [PubMed: 10516284]

66. Pusztaszeri MP, Seelentag W, Bosman FT: Immunohistochemical expression of endothelial markers CD31, CD34, von Willebrand factor, and Fli-1 in normal human tissues. J Histochem Cytochem 54: 385–395, 2006 [PubMed: 16234507]

67. Pilling D, Fan T, Huang D, Kaul B, Gomer RH: Identification of markers that distinguish monocyte-derived fibrocytes from monocytes, macrophages, and fibroblasts. PLoS ONE 4: e7475, 2009 [PMCID: PMC2759556] [PubMed: 19834619]

68. Klco JM, Kulkarni S, Kreisel FH, Nguyen TD, Hassan A, Frater JL: Immunohistochemical analysis of monocytic leukemias: Usefulness of CD14 and Kruppel-like factor 4, a novel monocyte marker. Am J Clin Pathol 135: 720–730, 2011 [PubMed: 21502426]

69. Ilan N, Cheung L, Pinter E, Madri JA: Platelet-endothelial cell adhesion molecule-1 (CD31), a scaffolding molecule for selected catenin family members whose binding is mediated by different tyrosine and serine/threonine phosphorylation. J Biol Chem 275: 21435–21443, 2000 [PubMed: 10801826]

70. Hartmann J, Dragicevic E, Adelsberger H, Henning HA, Sumser M, Abramowitz J, Blum R, Dietrich A, Freichel M, Flockerzi V, Birnbaumer L, Konnerth A: TRPC3 channels are required for synaptic transmission and motor coordination. Neuron 59: 392–398, 2008 [PMCID: PMC2643468] [PubMed: 18701065]

71. Strutz F, Zeisberg M: Renal fibroblasts and myofibroblasts in chronic kidney disease. J Am Soc Nephrol 17: 2992–2998, 2006 [PubMed: 17035610]

72. Wolf G: Renal injury due to renin-angiotensin-aldosterone system activation of the transforming growth factor-beta pathway. Kidney Int 70: 1914–1919, 2006 [PubMed: 16985515]

73. Ruiz-Ortega M, Rupérez M, Esteban V, Rodríguez-Vita J, Sánchez-López E, Carvajal G, Egido J: Angiotensin II: A key factor in the inflammatory and fibrotic response in kidney diseases. Nephrol Dial Transplant 21: 16–20, 2006 [PubMed: 16280370]

74. Pimentel JL, Jr., Montero A, Wang S, Yosipiv I, el-Dahr S, Martínez-Maldonado M: Sequential changes in renal expression of renin-angiotensin system genes in acute unilateral ureteral obstruction. Kidney Int 48: 1247–1253, 1995 [PubMed: 8569086]

75. Satoh M, Kashihara N, Yamasaki Y, Maruyama K, Okamoto K, Maeshima Y, Sugiyama H, Sugaya T, Murakami K, Makino H: Renal interstitial fibrosis is reduced in angiotensin II type 1a receptor-deficient mice. J Am Soc Nephrol 12: 317–325, 2001 [PubMed: 11158221]

76. Pimentel JL, Jr., Wang S, Martinez-Maldonado M: Regulation of the renal angiotensin II receptor gene in acute unilateral ureteral obstruction. Kidney Int 45: 1614–1621, 1994 [PubMed: 7933808]

77. Ishidoya S, Morrissey J, McCracken R, Reyes A, Klahr S: Angiotensin II receptor antagonist ameliorates renal tubulointerstitial fibrosis caused by unilateral ureteral obstruction. Kidney Int 47: 1285–1294, 1995 [PubMed: 7637258]

78. Abramowitz J, Birnbaumer L: Physiology and pathophysiology of canonical transient receptor potential channels. FASEB J 23: 297–328, 2009 [PMCID: PMC2630793] [PubMed: 18940894]

79. Earley S, Gonzales AL: (Sub)family feud: Crosstalk between TRPC channels in vascular smooth muscle cells during vasoconstrictor agonist stimulation. J Physiol 588: 3637–3638, 2010 [PMCID: PMC2998216] [PubMed: 20889491]

80. Hopf FW, Turner PR, Denetclaw WF, Jr., Reddy P, Steinhardt RA: A critical evaluation of resting intracellular free calcium regulation in dystrophic mdx muscle. Am J Physiol 271: C1325–C1339, 1996 [PubMed: 8897840]

81. Parekh AB, Penner R: Store depletion and calcium influx. Physiol Rev 77: 901–930, 1997 [PubMed: 9354808]

82. Numaga T, Nishida M, Kiyonaka S, Kato K, Katano M, Mori E, Kurosaki T, Inoue R, Hikida M, Putney JW, Jr., Mori Y: Ca2+ influx and protein scaffolding via TRPC3 sustain PKCbeta and ERK activation in B cells. J Cell Sci 123: 927–938, 2010 [PMCID: PMC2831761] [PubMed: 20179100]

83. Olson ER, Shamhart PE, Naugle JE, Meszaros JG: Angiotensin II-induced extracellular signal-regulated kinase 1/2 activation is mediated by protein kinase Cdelta and intracellular calcium in adult rat cardiac fibroblasts. Hypertension 51: 704–711, 2008 [PubMed: 18195168]

84. Schorb W, Conrad KM, Singer HA, Dostal DE, Baker KM: Angiotensin II is a potent stimulator of MAP-kinase activity in neonatal rat cardiac fibroblasts. J Mol Cell Cardiol 27: 1151–1160, 1995 [PubMed: 7473773]

85. Stockand JD, Meszaros JG: Aldosterone stimulates proliferation of cardiac fibroblasts by activating Ki-RasA and MAPK1/2 signaling. Am J Physiol Heart Circ Physiol 284: H176–H184, 2003 [PubMed: 12388314]

86. Liu Y: Cellular and molecular mechanisms of renal fibrosis. Nat Rev Nephrol 7: 684–696, 2011 [PMCID: PMC4520424] [PubMed: 22009250]

87. Davis J, Burr AR, Davis GF, Birnbaumer L, Molkentin JD: A TRPC6-dependent pathway for myofibroblast transdifferentiation and wound healing in vivo. Dev Cell 23: 705–715, 2012 [PMCID: PMC3505601] [PubMed: 23022034]

88. Carter AB, Monick MM, Hunninghake GW: Both Erk and p38 kinases are necessary for cytokine gene transcription. Am J Respir Cell Mol Biol 20: 751–758, 1999 [PubMed: 10101008]

89. Nagai Y, Miyata K, Sun GP, Rahman M, Kimura S, Miyatake A, Kiyomoto H, Kohno M, Abe Y, Yoshizumi M, Nishiyama A: Aldosterone stimulates collagen gene expression and synthesis via activation of ERK1/2 in rat renal fibroblasts. Hypertension 46: 1039–1045, 2005 [PubMed: 16087786]

90. Rokosova B, Bentley JP: Effect of calcium on cell proliferation and extracellular matrix synthesis in arterial smooth muscle cells and dermal fibroblasts. Exp Mol Pathol 44: 307–317, 1986 [PubMed: 3720919]

91. Zhu B, Wang YJ, Zhu CF, Lin Y, Zhu XL, Wei S, Lu Y, Cheng XX: Triptolide inhibits extracellular matrix protein synthesis by suppressing the Smad2 but not the MAPK pathway in TGF-beta1-stimulated NRK-49F cells. Nephrol Dial Transplant 25: 3180–3191, 2010 [PubMed: 20466671]

92. Earley S: Molecular diversity of receptor operated channels in vascular smooth muscle: A role for heteromultimeric TRP channels? Circ Res 98: 1462–1464, 2006 [PubMed: 16794194]

93. Gudermann T, Hofmann T, Mederos y Schnitzler M, Dietrich A: Activation, subunit composition and physiological relevance of DAG-sensitive TRPC proteins. Novartis Found Symp 258: 103–118, 2004 [PubMed: 15104178]

94. Goel M, Sinkins WG, Schilling WP: Selective association of TRPC channel subunits in rat brain synaptosomes. J Biol Chem 277: 48303–48310, 2002 [PubMed: 12377790]

95. Dietrich A, Mederos Y Schnitzler M, Gollasch M, Gross V, Storch U, Dubrovska G, Obst M, Yildirim E, Salanova B, Kalwa H, Essin K, Pinkenburg O, Luft FC, Gudermann T, Birnbaumer L: Increased vascular smooth muscle contractility in TRPC6-/- mice. Mol Cell Biol 25: 6980–6989, 2005 [PMCID: PMC1190236] [PubMed: 16055711]

96. Li SW, Westwick J, Poll CT: Receptor-operated Ca2+ influx channels in leukocytes: A therapeutic target? Trends Pharmacol Sci 23: 63–70, 2002 [PubMed: 11830262]

97. Nilius B, Owsianik G, Voets T, Peters JA: Transient receptor potential cation channels in disease. Physiol Rev 87: 165–217, 2007 [PubMed: 17237345]

98. Storch U, Forst AL, Philipp M, Gudermann T, Mederos y Schnitzler M: Transient receptor potential channel 1 (TRPC1) reduces calcium permeability in heteromeric channel complexes. J Biol Chem 287: 3530–3540, 2012 [PMCID: PMC3271006] [PubMed: 22157757]

99. Kuwahara K, Wang Y, McAnally J, Richardson JA, Bassel-Duby R, Hill JA, Olson EN: TRPC6 fulfills a calcineurin signaling circuit during pathologic cardiac remodeling. J Clin Invest 116: 3114–3126, 2006 [PMCID: PMC1635163] [PubMed: 17099778]

100. Pat B, Yang T, Kong C, Watters D, Johnson DW, Gobe G: Activation of ERK in renal fibrosis after unilateral ureteral obstruction: Modulation by antioxidants. Kidney Int 67: 931–943, 2005 [PubMed: 15698432]

101. Rodríguez-Peña AB, Grande MT, Eleno N, Arévalo M, Guerrero C, Santos E, López-Novoa JM: Activation of Erk1/2 and Akt following unilateral ureteral obstruction. Kidney Int 74: 196–209, 2008 [PubMed: 18449171]

102. Fu P, Liu F, Su S, Wang W, Huang XR, Entman ML, Schwartz RJ, Wei L, Lan HY: Signaling mechanism of renal fibrosis in unilateral ureteral obstructive kidney disease in ROCK1 knockout mice. J Am Soc Nephrol 17: 3105–3114, 2006 [PubMed: 17005937]

103. Johnson DW, Saunders HJ, Baxter RC, Field MJ, Pollock CA: Paracrine stimulation of human renal fibroblasts by proximal tubule cells. Kidney Int 54: 747–757, 1998 [PubMed: 9734599]

104. Johnson DW, Saunders HJ, Brew BK, Ganesan A, Baxter RC, Poronnik P, Cook DI, György AZ, Field MJ, Pollock CA: Human renal fibroblasts modulate proximal tubule cell growth and transport via the IGF-I axis. Kidney Int 52: 1486–1496, 1997 [PubMed: 9407494]

105. Johnson DW, Saunders HJ, Johnson FJ, Huq SO, Field MJ, Pollock CA: Cyclosporin exerts a direct fibrogenic effect on human tubulointerstitial cells: Roles of insulin-like growth factor I, transforming growth factor beta1, and platelet-derived growth factor. J Pharmacol Exp Ther 289: 535–542, 1999 [PubMed: 10087047]

106. Kelynack KJ, Hewitson TD, Nicholls KM, Darby IA, Becker GJ: Human renal fibroblast contraction of collagen I lattices is an integrin-mediated process. Nephrol Dial Transplant 15: 1766–1772, 2000

[PubMed: 11071963]

107. Masterson R, Hewitson TD, Kelynack K, Martic M, Parry L, Bathgate R, Darby I, Becker G: Relaxin down-regulates renal fibroblast function and promotes matrix remodelling in vitro. Nephrol Dial Transplant 19: 544–552, 2004 [PubMed: 14767007]

108. Shivakumar K, Kumaran C: L-type calcium channel blockers and EGTA enhance superoxide production in cardiac fibroblasts. J Mol Cell Cardiol 33: 373–377, 2001 [PubMed: 11162140]

109. Soldatov NM: Molecular diversity of L-type Ca2+ channel transcripts in human fibroblasts. Proc Natl Acad Sci U S A 89: 4628–4632, 1992 [PMCID: PMC49136] [PubMed: 1316612]

110. Yang S, Huang XY: Ca2+ influx through L-type Ca2+ channels controls the trailing tail contraction in growth factor-induced fibroblast cell migration. J Biol Chem 280: 27130–27137, 2005 [PubMed: 15911622]

111. Zhu DL, Hérembert T, Caruelle D, Caruelle JP, Marche P: Involvement of calcium channels in fibroblast growth factor-induced activation of arterial cells in spontaneously hypertensive rats. J Cardiovasc Pharmacol 23: 395–400, 1994 [PubMed: 7515982]

112. Grynkiewicz G, Poenie M, Tsien RY: A new generation of Ca2+ indicators with greatly improved fluorescence properties. J Biol Chem 260: 3440–3450, 1985 [PubMed: 3838314]

113. Cerella C, Coppola S, Maresca V, De Nicola M, Radogna F, Ghibelli L: Multiple mechanisms for hydrogen peroxide-induced apoptosis. Ann N Y Acad Sci 1171: 559–563, 2009 [PubMed: 19723104]

114. McKeague AL, Wilson DJ, Nelson J: Staurosporine-induced apoptosis and hydrogen peroxide-induced necrosis in two human breast cell lines. Br J Cancer 88: 125–131, 2003 [PMCID: PMC2376787] [PubMed: 12556971]

Figures and Tables

Figure 1.

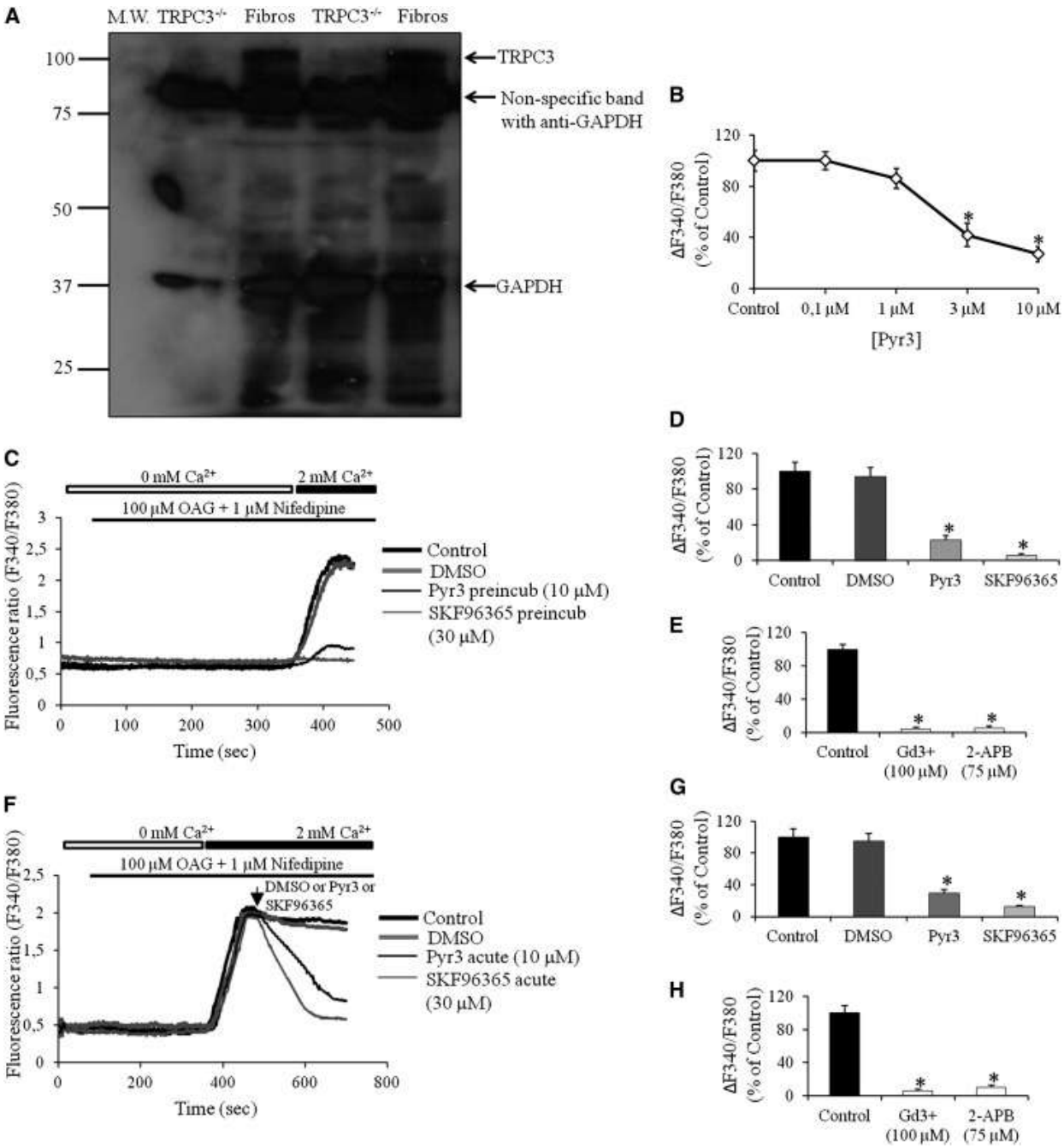

Open in a separate window

TRPC3 is expressed and functional in adult renal fibroblasts. (A) Western blot of TRPC3 in rat renal fibroblasts and kidneys of TRPC3$^{-/-}$ mice used as a negative control, with GAPDH as an internal control (n=12 rats). TRPC3-specific protein band is indicated by an arrow. (B) Amplitude of fura-2 signal reported as the percentage of control showing dose-dependent effect of pyr3 on OAG-induced Ca^{2+} entry in renal fibroblasts (n=35 cells from five rats for each condition). (C and F) Representative recordings of fura-2 emission ratio (F340/F380) in the renal fibroblasts showing the effect of pyr3 on Ca^{2+} entries. (D, E, G, and H) Quantifications of fura-2 amplitudes (ΔF340/F380) in the various conditions (n=10–14 cells from four rats for each condition). Data for fura-2 amplitudes are represented as mean percentage of controls±SEMs. Fibros, fibroblasts; GAPDH, glyceraldehyde-3-phosphate dehydrogenase; MW, molecular weight. *P<0.01 versus control and DMSO.

Figure 2.

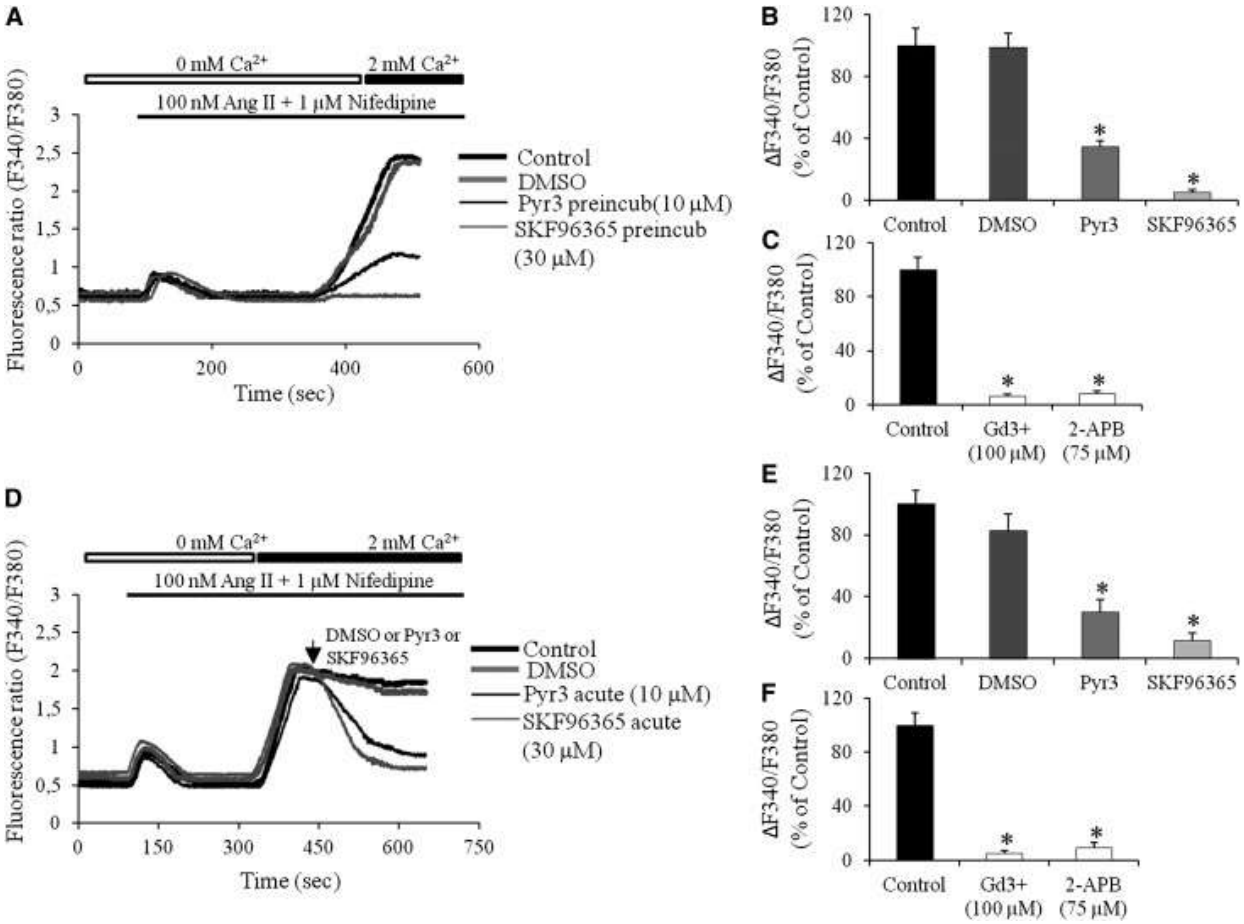

Open in a separate window

TRPC3 inhibition blocks Ang II-induced Ca^{2+} entry in adult renal fibroblasts. (A and D) Representative recordings of fura-2 emission ratio (F340/F380) in the renal fibroblasts. (B, C, E, and F) Quantifications of fura-2 amplitudes (ΔF340/F380) in the various conditions showing the effect of TRPC3 blockade on Ca^{2+} influx (n=10–14 cells from four rats for each condition). Data for fura-2 amplitudes are represented as mean percentage of controls±SEMs. *P<0.01 versus control and DMSO.

Figure 3.

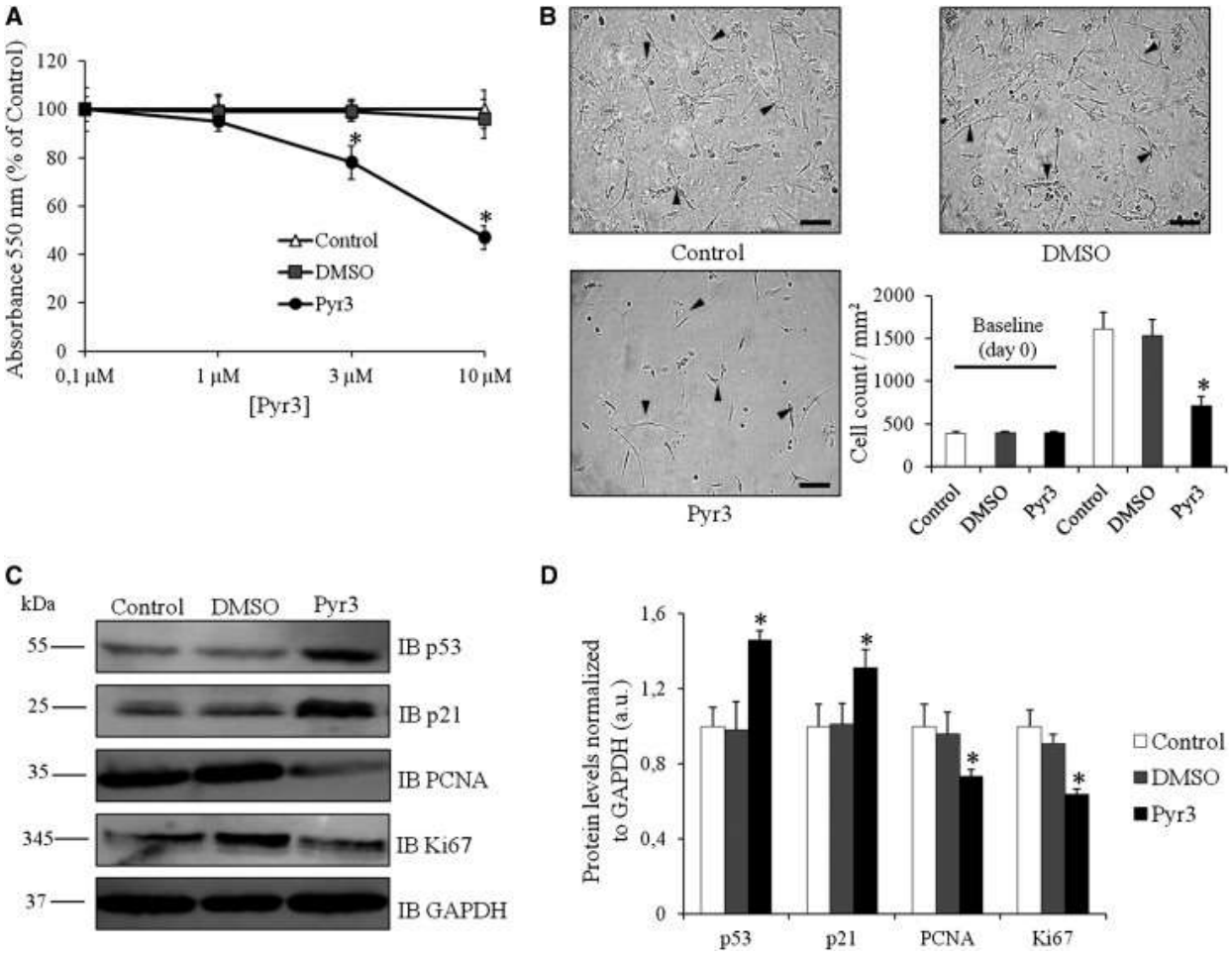

Open in a separate window

TRPC3 inhibition blocks renal fibroblasts proliferation. (A) Renal fibroblasts proliferation estimated by MTT assay after 48 hours of treatment with DMSO or different concentrations of pyr3; absorbance at 550 nm. (B) Representative light microscopy photographs showing the effect of 10 µm pyr3 on renal fibroblasts proliferation and histograms representing cell numbers per square millimeter of culture well in each condition before (baseline) and after treatments. (C) Western blots showing the regulation of cell cycle regulators in renal fibroblasts treated with either DMSO or pyr3. (D) Studied proteins normalized to GAPDH. Small arrows show individual fibroblasts in B. n=16 cultures from eight rats for each condition. Data are represented as means±SEMs. a.u., arbitrary units; GAPDH, glyceraldehyde-3-phosphate dehydrogenase; IB, immunoblot. Magnification, ×100. Scale bars, 50 μm. *P<0.05 versus control and DMSO.

Figure 4.

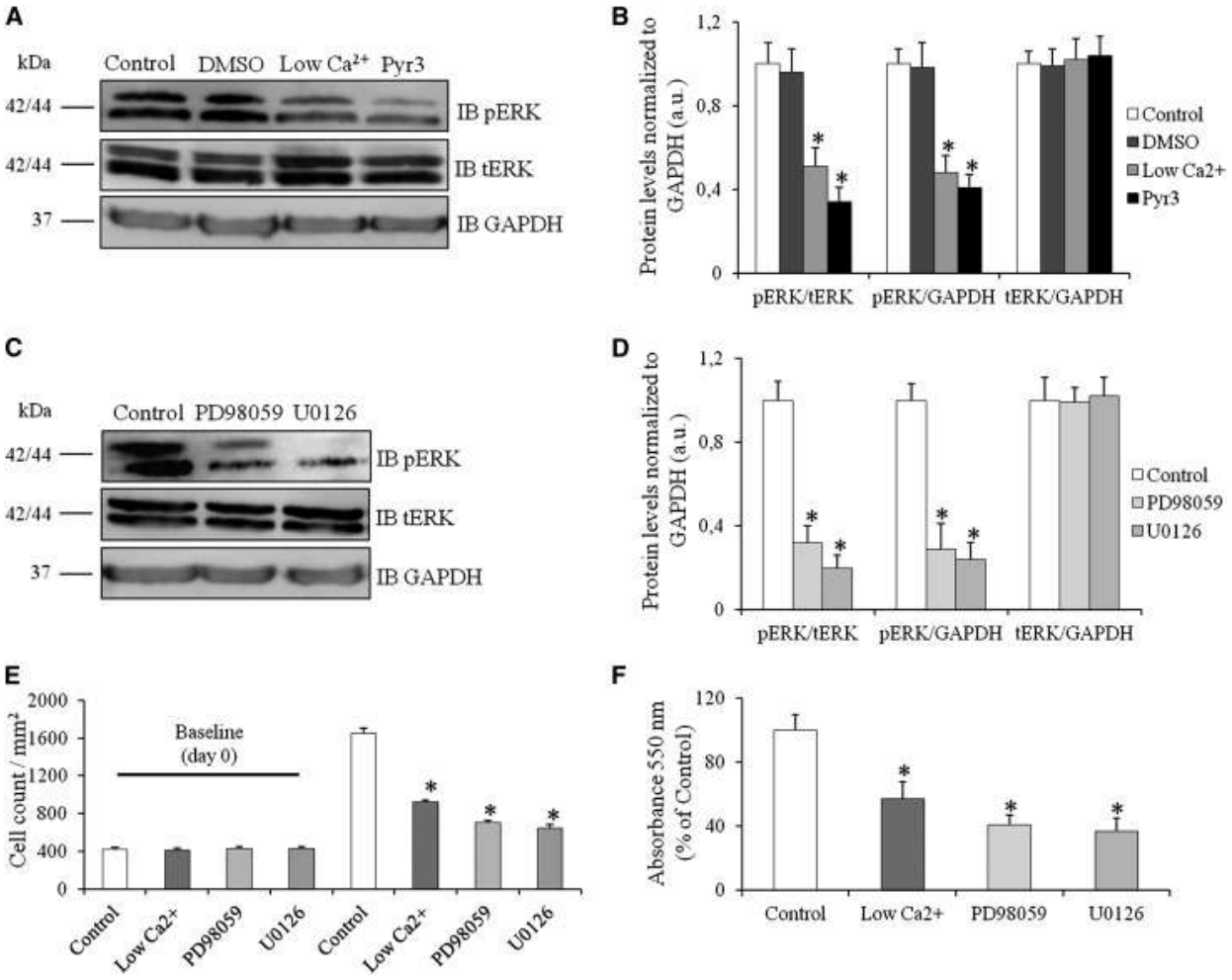

Open in a separate window

TRPC3-mediated Ca^{2+}-dependent ERK1/2 activation. (A) Western blots and (B) relative quantifications of the effect of TRPC3 and Ca^{2+} influx blockade (10 μM pyr3 and low extracellular Ca^{2+}) on the phosphorylation of ERK1/2. (C and D) Western blots and quantifications showing the effects of mitogen-activated protein kinase (MAPK) pathway inhibitors on ERK1/2 phosphorylation. GAPDH is used as an internal control. (E and F) Effects of low extracellular Ca^{2+} and MAPK inhibitors on the proliferation of renal fibroblasts revealed by cell count per millimeter^2 and reactivity to MTT assay, respectively; baseline counting was done at the start of the culture (day 0), and absorbance was at 550 nm. n=16 cultures from eight rats for each condition. Data are represented as means±SEMs. a.u., arbitrary units; GAPDH, glyceraldehyde-3-phosphate dehydrogenase; IB, immunoblot. *P<0.05 versus control and DMSO.

Figure 5.

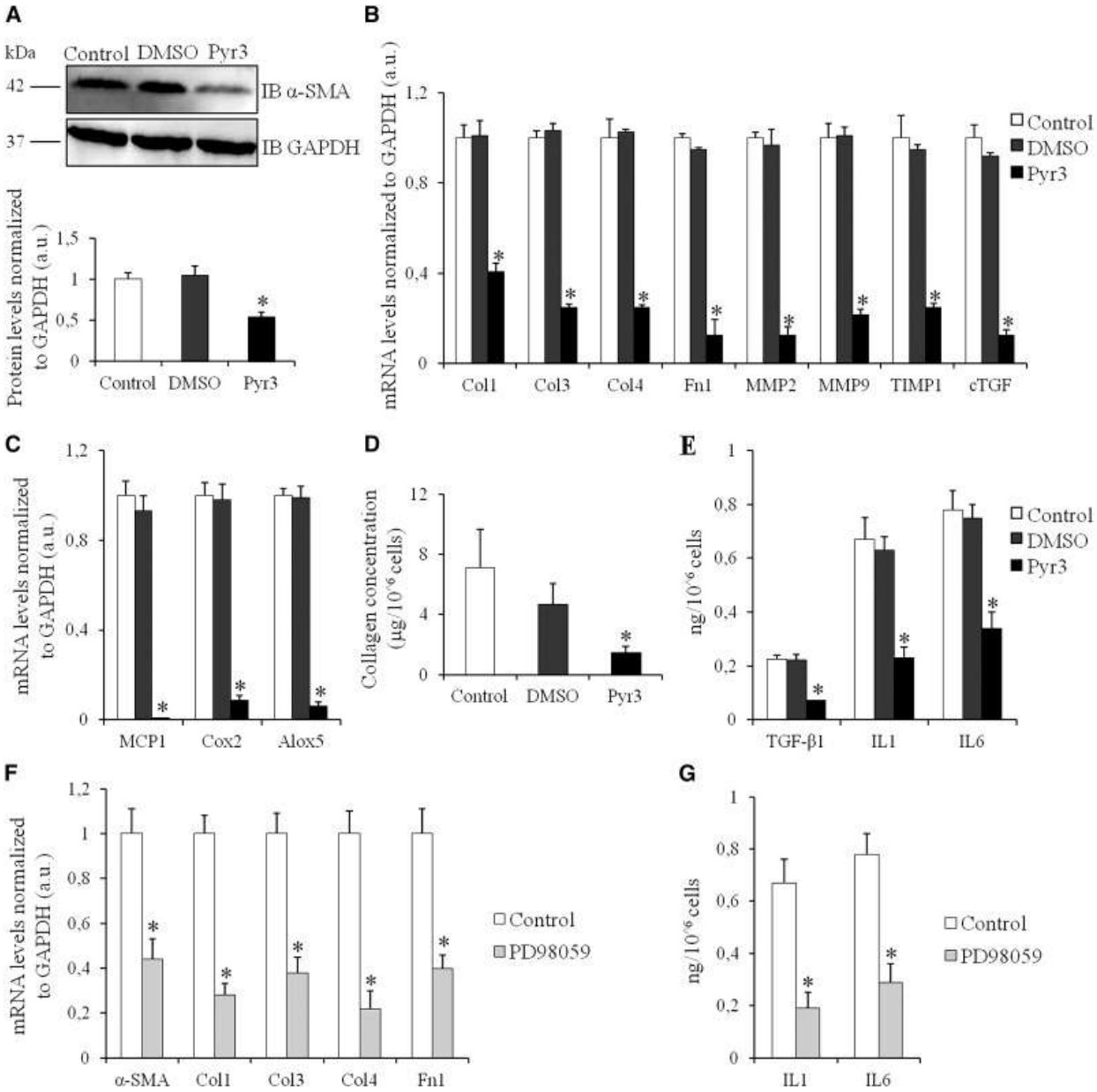

Open in a separate window

Suppression of fibroblasts differentiation and fibrotic and inflammatory phenotype with TRPC3 blockade. (A) Western blots and quantifications of fibroblasts α-SMA expression with pyr3 compared with control and DMSO. GAPDH was used as an internal control. (B and C) Gene expressions of fibrotic and inflammatory markers in fibroblasts under pyr3 treatment versus control and DMSO, respectively. GAPDH was used as a housekeeping gene. (D) Fibroblasts collagen synthesis measured by sircol assay under TRPC3 blockade compared with DMSO-treated and control cells; collagen concentrations are reported as micrograms per 10^6 cells. (E) Fibrotic and inflammatory cytokines secretions by pyr3-treated renal fibroblasts compared with DMSO-treated and control cells; concentrations are reported as nanograms per 10^6 cells. (F and G) Relative mRNA levels of fibrotic components reported to GAPDH and cytokines secretions (nanograms per 10^6 cells) of renal fibroblasts treated with PD98059. n=16 cultures from eight rats for each condition. Data are represented as means±SEMs. a.u., arbitrary units; GAPDH, glyceraldehyde-3-phosphate dehydrogenase; IB, immunoblot. *P<0.01 versus control and DMSO.

Figure 6.

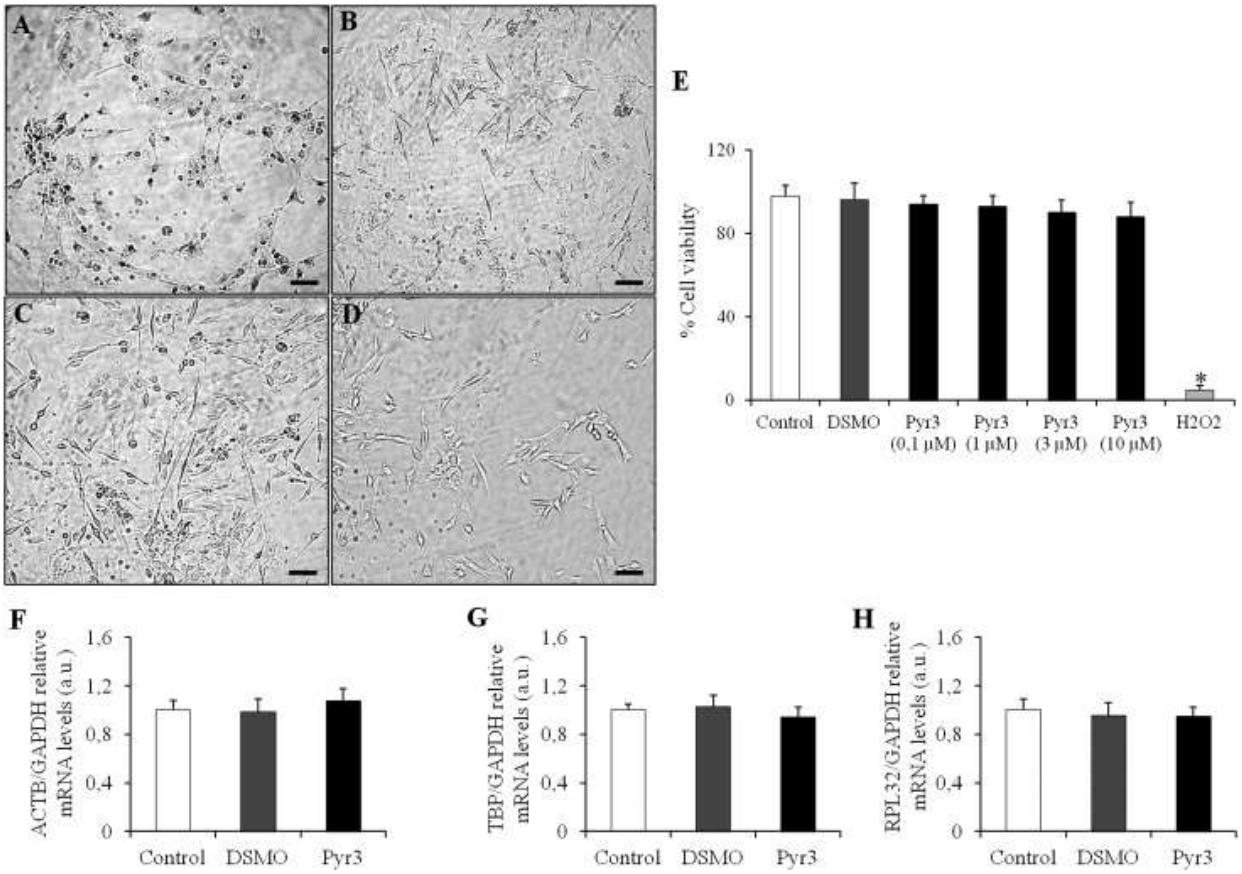

Noncytotoxic effects of pyr3 on rat renal fibroblasts. Representative light microscopy photographs showing Trypan blue exclusion test on renal fibroblasts treated with (A) H_2O_2, (B) nontreated control, (C) DMSO, and (D) pyr3 (10 μM). (E) Cell viability with different concentrations of pyr3 was reported as a percentage to control. (F–H) Housekeeping genes expressions normalized to GAPDH. n=16 cultures from eight rats for each condition. Data are represented as means±SEMs. a.u., arbitrary units; GAPDH, glyceraldehyde-3-phosphate dehydrogenase. Magnification, ×100. Scale bars, 50 μm. *P<0.001 H_2O_2 versus control.

Figure 7.

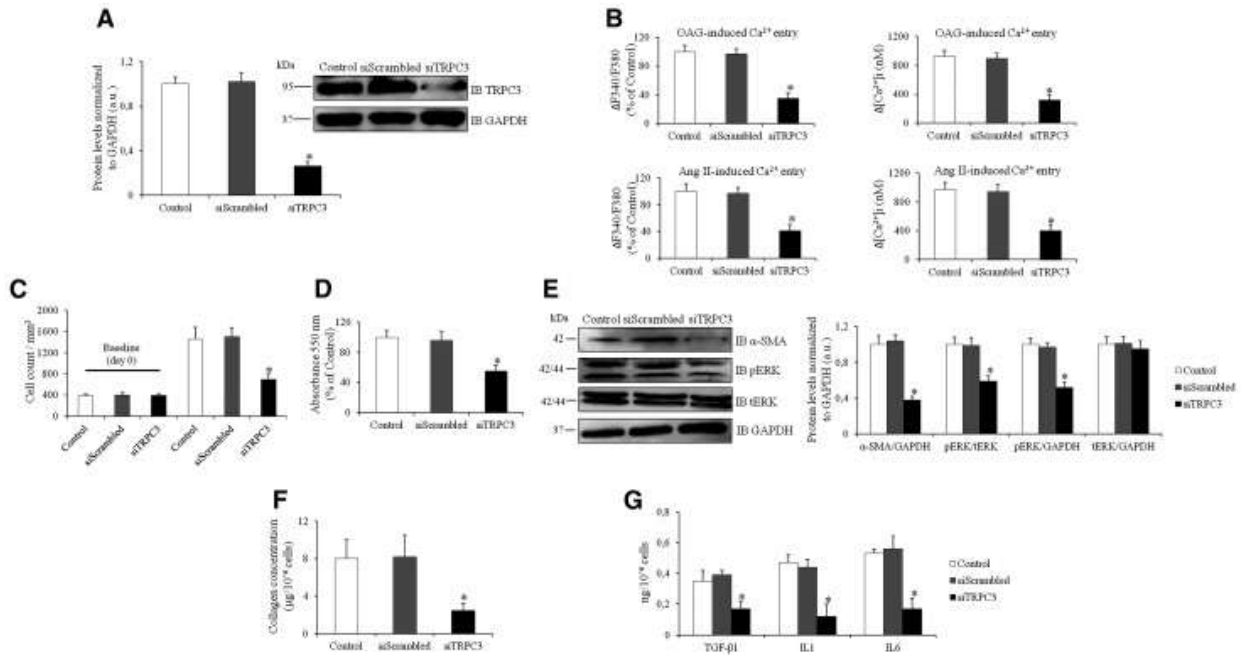

TRPC3 knockdown inhibits fibroblast activation, proliferation, and fibrotic and inflammatory phenotypes. (A) Western blots and quantifications showing the efficient knockdown of TRPC3 with specific siRNA. (B) Quantifications of (left panels) fura-2 amplitudes (ΔF340/F380) and (right panels) intracellular Ca^{2+} concentrations $\Delta[Ca^{2+}]i$ showing the effect of siTRPC3 on OAG- and Ang II-induced Ca^{2+} entries in renal fibroblasts compared with control and siScrambled-transfected cells. (C) Histograms representing cell numbers per square millimeter of culture well at day 0 of culture (baseline) and after 48 hours transfection (day 5) with either siTRPC3 or siScrambled. (D) Proliferation MTT assay showing the decrease in cell proliferation with TRPC3 knockdown. (E) Western blots and quantifications showing the effect of siTRPC3 on α-SMA expression and ERK1/2 phosphorylation in renal fibroblasts. (F and G) Effects of TRPC3 knockdown on collagen and fibrotic/inflammatory cytokines synthesis measured with sircol assay and ELISA, respectively, and reported as micrograms per 10^6 cells and nanograms per 10^6 cells, respectively. GAPDH was used as an internal control in all Western blots. n=16 cultures from eight rats for each condition. Data are represented as means±SEMs. a.u., arbitrary units; GAPDH, glyceraldehyde-3-phosphate dehydrogenase; IB, immunoblot. *P<0.05 versus siScrambled and control.

Figure 8.

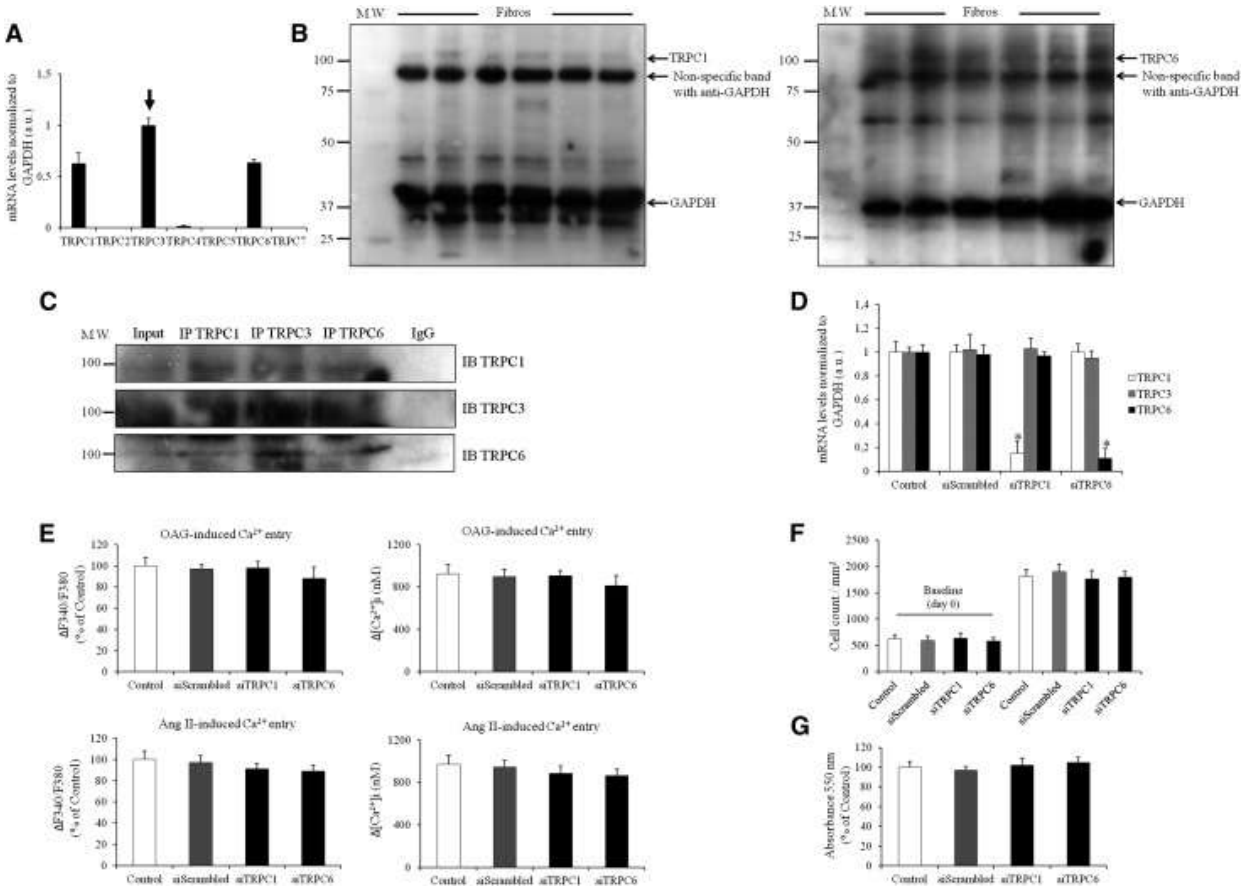

Characterization of the expression, subunit composition, and function of TRPC channel isoforms in rat renal fibroblasts. (A and B) Quantitative real-time PCR and Western blots of different TRPC channel isoforms present in renal fibroblasts; *n*=6 cultures from six rats for each condition. GAPDH was used as an internal control in all Western blots. The arrow in A shows the expression of TRPC3. (C) Presence of a macromolecular complex formed by TRPC1/TRPC3/TRPC6 in renal fibroblasts as revealed by coimmunoprecipitation of TRPC1, -3, and -6 with TRPC1, -3, and -6; *n*=6 cultures from six rats for each condition. Nonrelevant rabbit IgG was used a negative control. (D–G) TRPC1 and -6 are not implicated in OAG- and Ang II-induced Ca^{2+} entries in the studied cells, which is shown by specific channels knockdown. Specific individual TRPC channel knockdown was verified by quantitative real-time PCR, whereas proliferation was verified by cell counting and MTT assay; *n*=6 cultures from six rats for each condition. Quantifications of (E, left panels) fura-2 amplitudes (ΔF340/F380) and (E, right panels) intracellular Ca^{2+} concentrations $\Delta[Ca^{2+}]i$ are also presented (*n*=10–14 cells from four rats for each condition). a.u., arbitrary units; fibros, fibroblasts; GAPDH, glyceraldehyde-3-phosphate dehydrogenase; IB, immunoblot; IP, immunoprecipitation; MW, molecular weight. Data are represented as means±SEMs. **P*<0.01 versus control.

Figure 9.

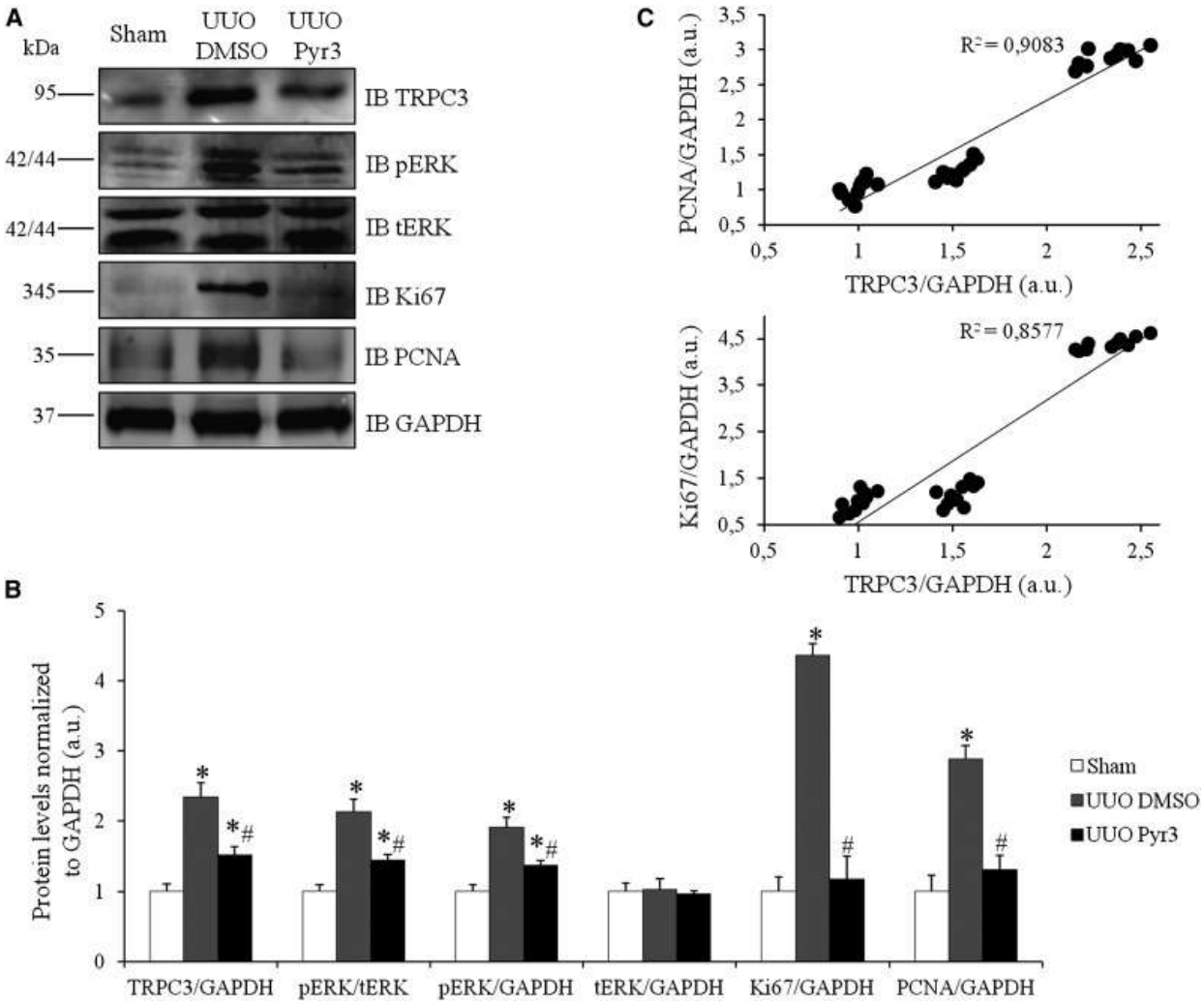

Open in a separate window

In vivo pyr3 treatment prevents TRPC3 upregulation, ERK phosphorylation, and renal fibroblasts proliferation in UUO kidneys. (A and B) Western blots and quantifications showing the effect of pyr3 *in vivo* administration on levels of TRPC3, phospho-ERK, and cell cycle regulators Ki67 and PCNA in renal fibroblasts of obstructed kidneys (UUO) compared with DMSO-treated and sham animals. (C) Correlation of TRPC3 expression with cell cycle proteins Ki67 and PCNA. GAPDH was used as an internal control. n=30 rats (10 rats in each group). Data are represented as means±SEMs. a.u., arbitrary units; GAPDH, glyceraldehyde-3-phosphate dehydrogenase; IB, immunoblot. *P<0.05 versus sham; #P<0.05 versus UUO DMSO.

Figure 10.

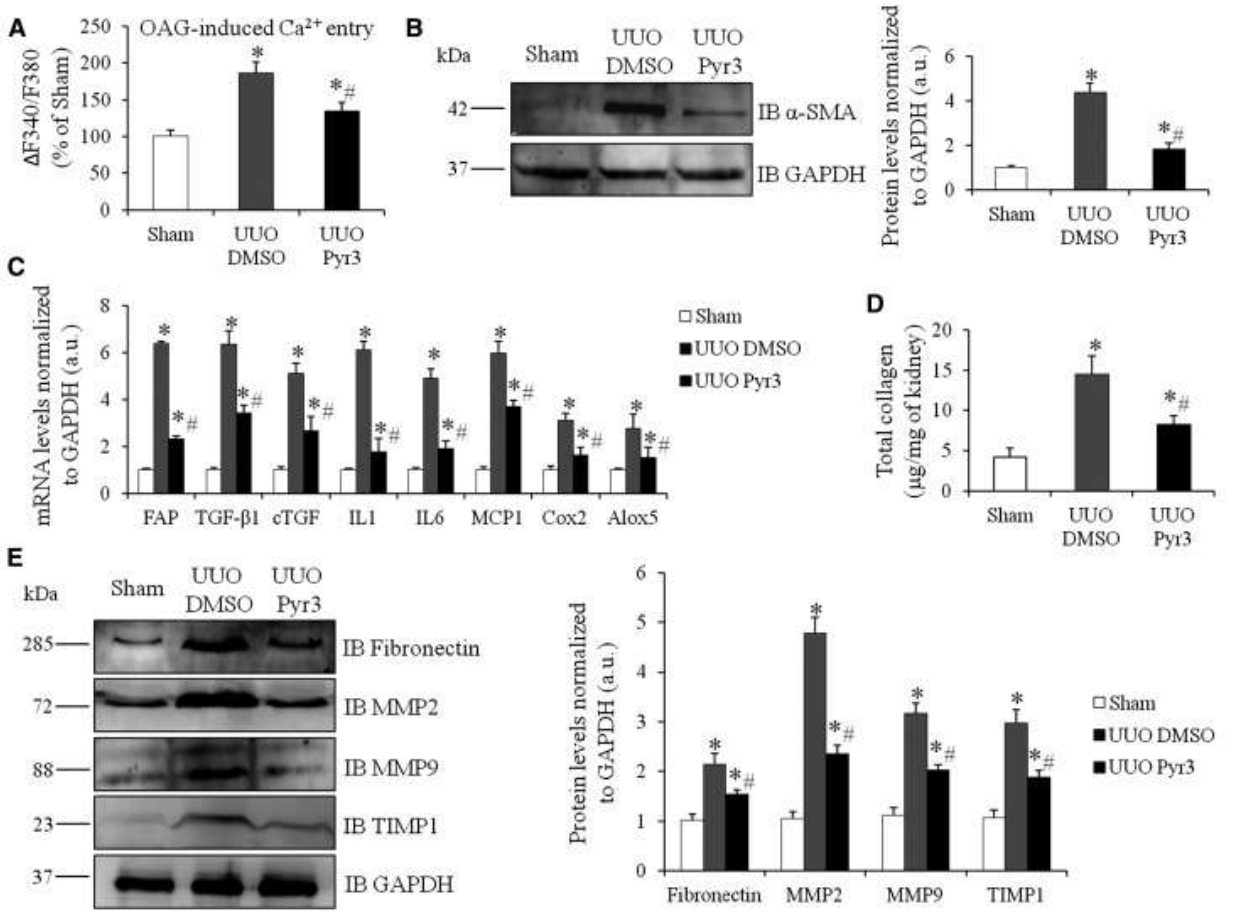

Open in a separate window

TRPC3 blockade inhibits fibroblast activation and ECM remodeling in UUO kidneys. (A) Quantifications of fura-2 amplitudes (*Δ*F340/F380) showing the effect of pyr3 treatment on OAG-induced Ca^{2+} entry in freshly isolated UUO renal fibroblasts. (B) Western blots and quantifications of *α*-SMA expression in renal fibroblasts of the different rat groups. (C) Gene expressions of fibroblast activation markers as well as fibrotic and inflammatory cytokines of these same cells. (D) Total collagen measurement by sircol assay in kidney sections reported as micrograms per milligram of kidney in the different animal groups. (E) Western blots and quantifications of different ECM components in kidney sections of the different groups. GAPDH was used as a housekeeping gene in all mRNA expressions and an internal control in all Western blots. *n*=30 rats (10 rats in each group). Data are represented as means±SEMs. a.u., arbitrary units; GAPDH, glyceraldehyde-3-phosphate dehydrogenase; IB, immunoblot. **P*<0.05 versus sham; $^{\#}$*P*<0.05 versus UUO DMSO.

Figure 11.

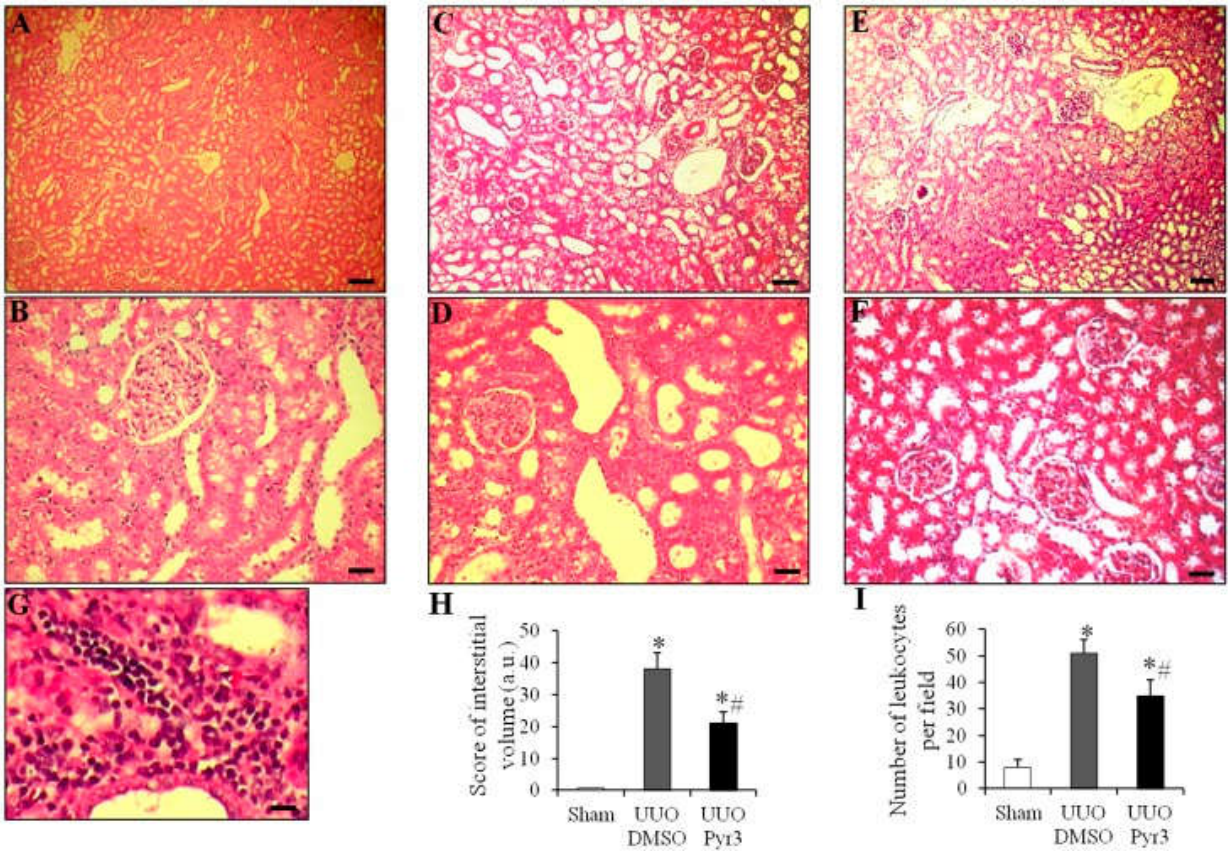

TRPC3 inhibition ameliorates histologic damage of the UUO kidneys. Representative microphotographs of left renal sections stained with hematoxylin-eosin showing (A and B) sham, (C and D) UUO DMSO, and (E and F) UUO pyr3 kidneys. (G) Leukocyte infiltration in different zones of the UUO DMSO kidneys. (H and I) Histograms showing semiquantitative scores of interstitial volume and numbers of infiltrating leukocytes per section field in the different kidneys. All histologic sections are 4-μm thick. n=6 sections for each rat from three groups. Data are represented as means±SEMs. a.u., arbitrary units. Magnification, ×100 in A, C, and E; ×400 for B, D, F, and G. Scale bars, 50 μM in A, C, and E; 12 μM in B, D, F, and G. *P<0.05 versus sham; $^{\#}P$<0.05 versus UUO DMSO.

Figure 12.

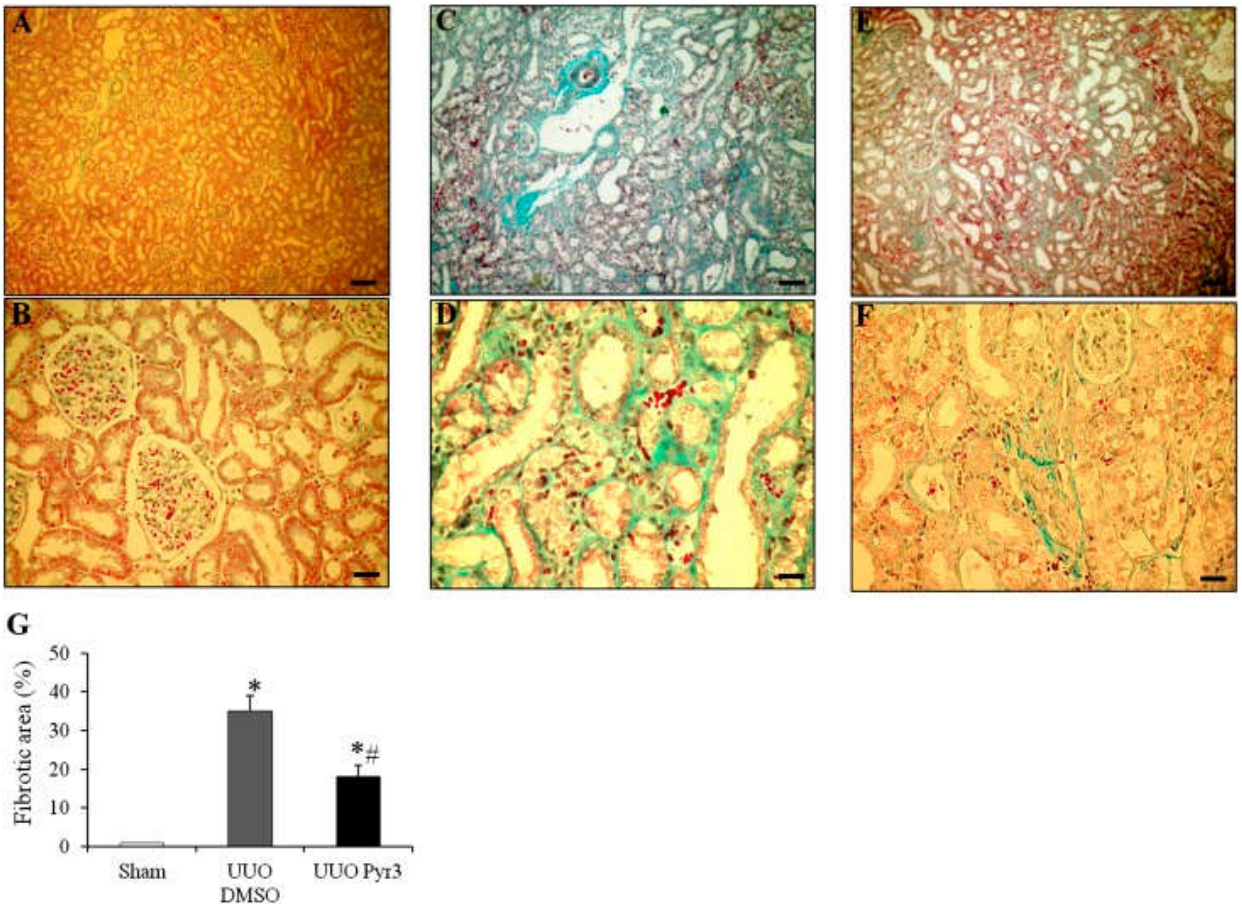

Open in a separate window

TRPC3 inhibition improves tubulointerstitial fibrosis in the UUO kidneys. Representative microphotographs of left renal sections stained with Masson's trichrome showing (A and B) sham, (C and D) UUO DMSO, and (E and F) UUO pyr3 kidneys. (G) Histogram showing semiquantitative scores of tubulointerstitial fibrosis in the different kidneys. All histologic sections are 4-μm thick. n=6 sections for each rat from three groups. Data are represented as means±SEMs. Magnification, ×100 in A, C, and E; ×400 in B, D, and F. Scale bars, 50 μM in A, C, and E; 12 μM in B, D, and F. *P<0.05 versus sham; $^{\#}P$<0.05 versus UUO DMSO.

Figure 13.

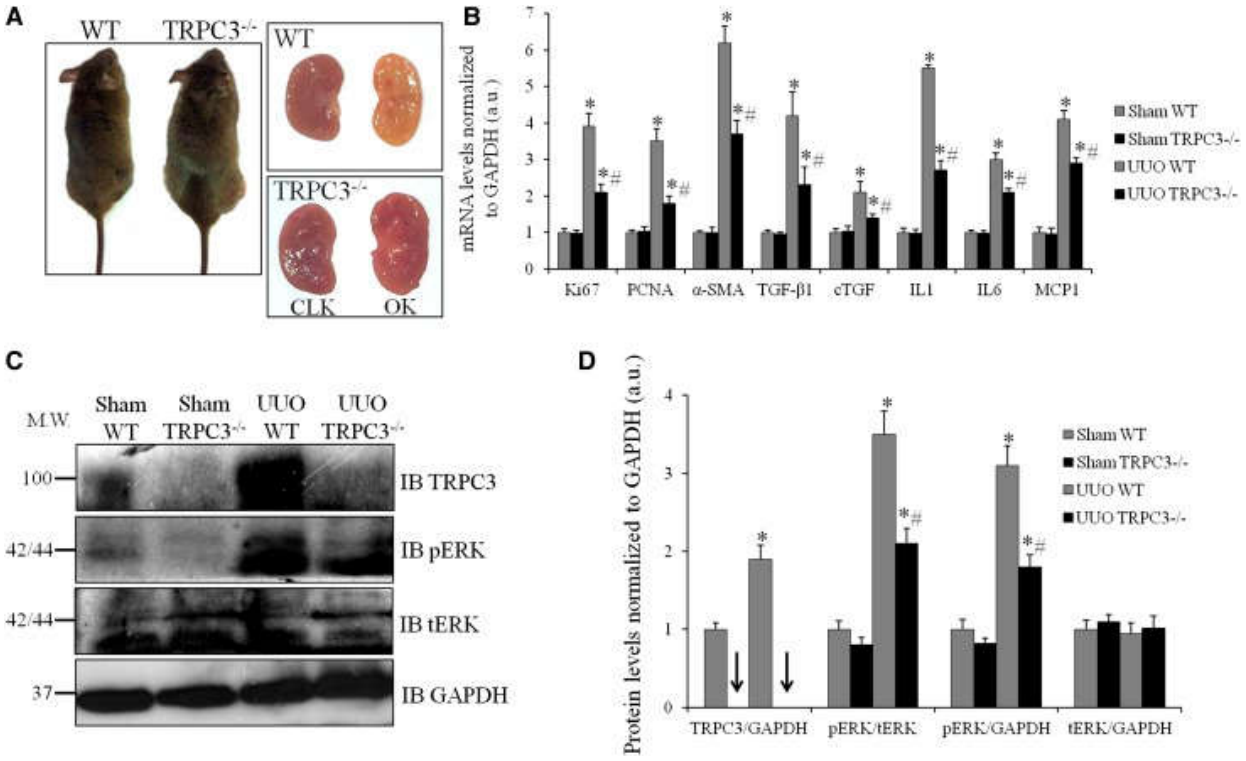

Renal fibroblasts of TRPC3$^{-/-}$ mice show decreased ERK phosphorylation and reduced secretory profile after UUO. (A) Photographs of a TRPC3$^{-/-}$ mouse and a WT mouse. Gross appearance of WT and TRPC3$^{-/-}$ left obstructed and right contralateral kidneys cross-sections after 10 days of UUO. Note that the obstructed kidney of the TRPC3$^{-/-}$ mouse showed relatively intact kidney tissue (much less whitish and yellowish scar area than in WT). (B) Gene expressions of fibroblast proliferation markers as well as fibrotic and inflammatory cytokines of these same cells in the different mice groups. (C and D) Western blots and quantifications showing the effect of TRPC3 deletion in mice on levels of phospho-ERK in renal fibroblasts of obstructed kidneys (UUO) compared with WT animals. GAPDH was used as an internal control. Arrows show the absence of TRPC3 expression in TRPC3$^{-/-}$ mice. n=32 mice (8 mice in each group). Data are represented as means±SEMs. a.u., arbitrary units; CLK, contralateral kidney; GAPDH, glyceraldehyde-3-phosphate dehydrogenase; IB, immunoblot; MW, molecular weight; OK, obstructed kidney. *P<0.01 versus sham WT and sham TRPC3$^{-/-}$; $^{\#}P$<0.01 versus UUO WT.

Figure 14.

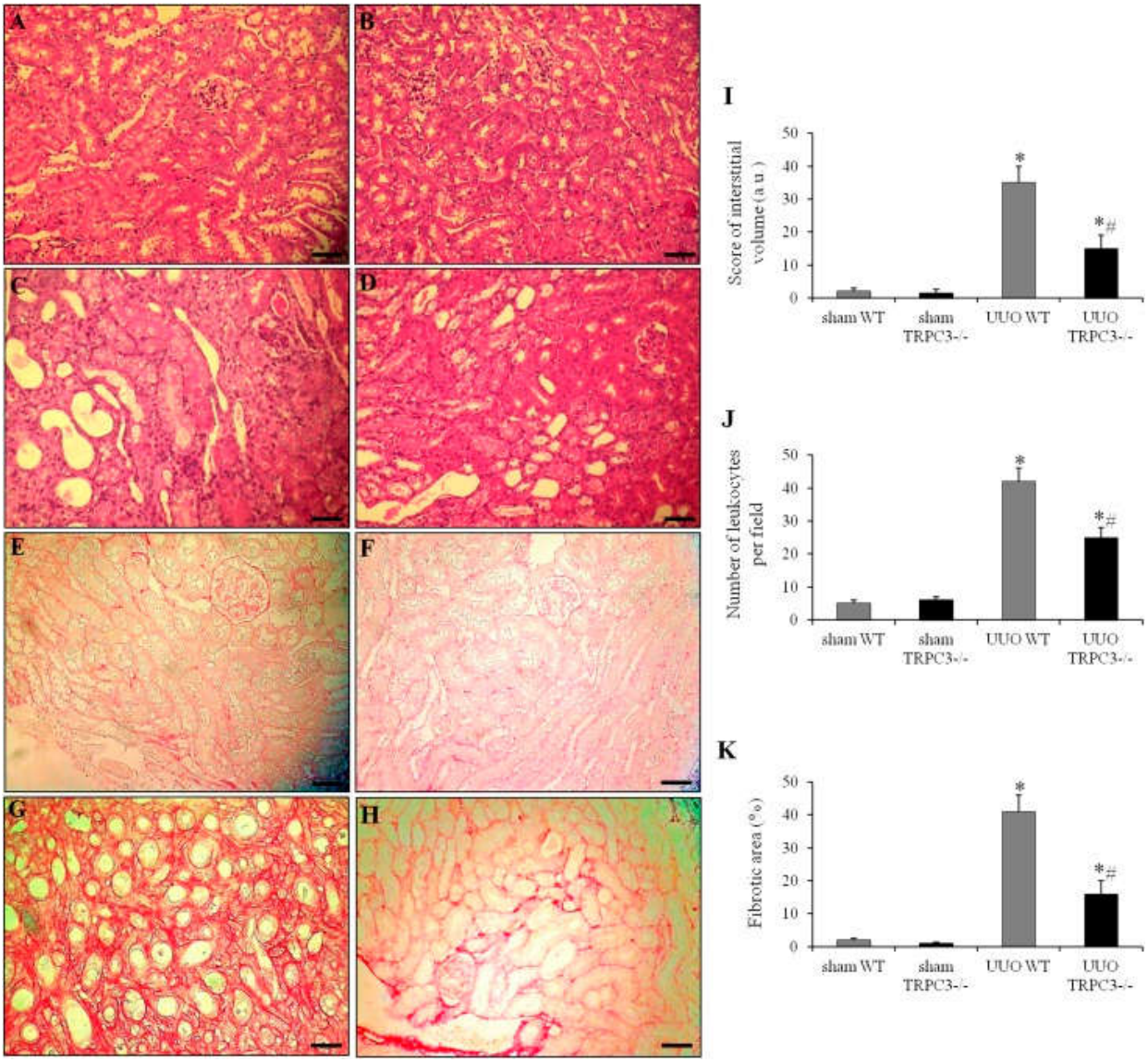

Open in a separate window

TRPC3$^{-/-}$ mice are protected against renal tissue deterioration and tubulointerstitial fibrosis after UUO. Representative microphotographs of left renal sections stained with (A–D) hematoxylin-eosin and (E–H) picrosirius red showing (A and E) sham WT, (B and F) sham TRPC3$^{-/-}$, (C and G) UUO WT, and (D and H) UUO TRPC3$^{-/-}$. (I–K) Histograms showing semiquantitative scores of interstitial volume, number of infiltrating leukocytes per section field, and fibrotic area (percentage) in the different kidneys. All histologic sections are 4-μm thick. n=6 sections for each mouse from four groups. Data are represented as means±SEMs. a.u., arbitrary units. Magnification, ×400. Scale bars, 12 μM. *P<0.05 versus sham WT and sham TRPC3$^{-/-}$; $^{\#}P$<0.05 versus UUO WT.

Figure 15.

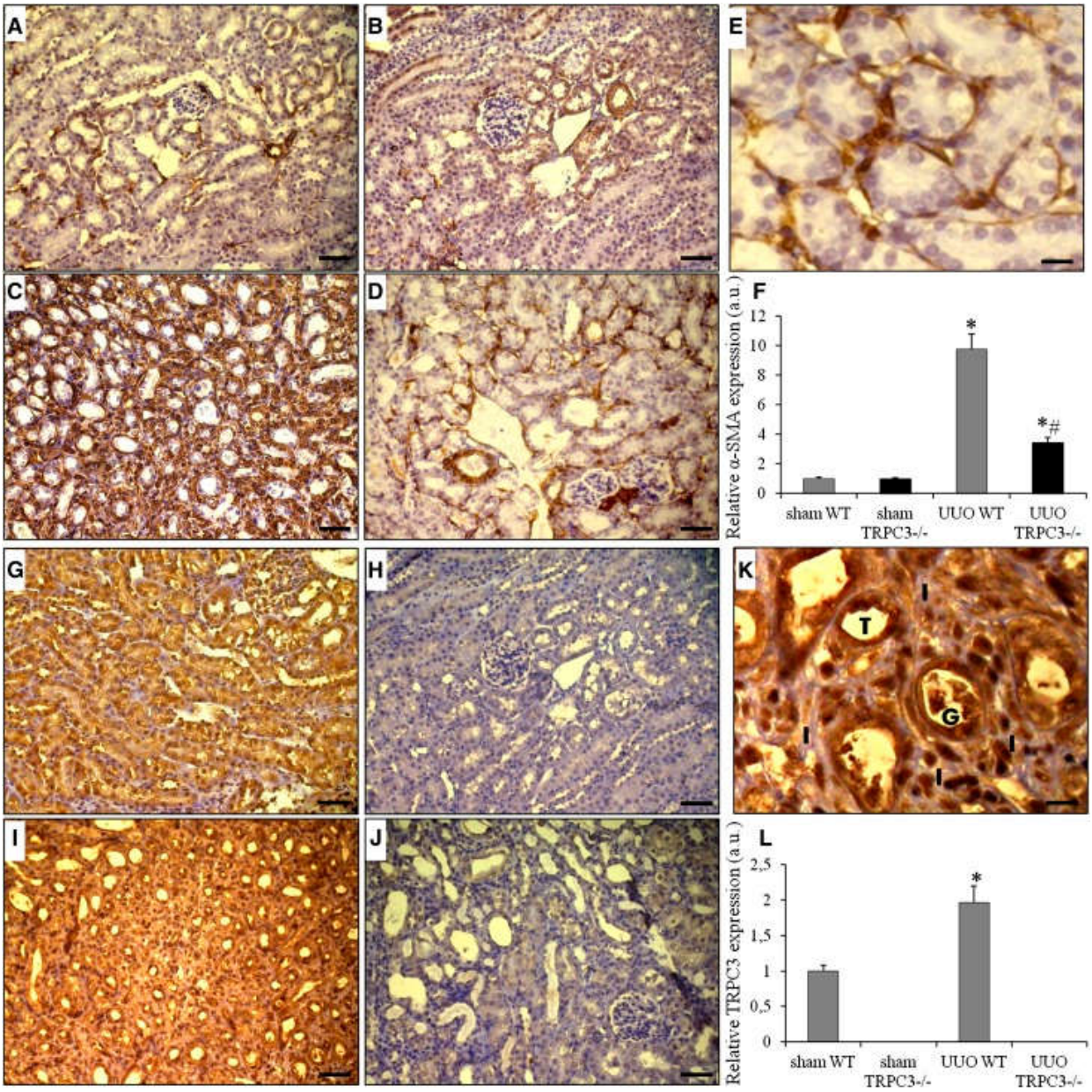

Open in a separate window

Upregulation of TRPC3 in the interstitium of the obstructed kidney. (A–E) Representative microphotographs and (F) quantifications of left renal sections labeled with (A–E) anti–α-SMA showing (A) sham WT, (B) sham TRPC3$^{-/-}$, (C) UUO WT, and (D) UUO TRPC3$^{-/-}$. (G–L) TRPC3 labeling and quantifications in left renal sections. All histologic sections are 4-μm thick. n=6 sections for each mouse from four groups. Data are represented as means±SEMs. a.u., arbitrary units; G, glomerulus; I, interstitium; T, tubule. Magnification, ×400 in A–D and G–J; ×600 in E and K. Scale bars, 12 μM in A–D and G–J; 8 μM in E and K. *P<0.05 versus sham WT and sham TRPC3$^{-/-}$; $^{\#}P$<0.05 versus UUO WT.